Studies on the development of novel non-alcoholic steatohepatitis (NASH) models using rats

YASUKA SAIGO

2023

Contents

List of Abbreviations

Abbreviation	Term
ALT	Alanine aminotransferase
AST	Aspartate aminotransferase
CCl_4	Carbon tetrachloride
CDAA	Choline-deficient L-amino-defined
CDX	Hydroxypropyl-β-cyclodextrin
CRN	Clinical Research Network
ER	Endoplasmic reticulum
FDA	Food and Drug Administration
FLIP	Fatty liver inhibition of progression
FXR	Farnesoid X receptor
GLU	Glucose
H&E	Hematoxylin Eosin
HFCC	High-fat, cholesterol, and cholic acid
HMG-CoA	Hydroxymethylglutaryl-CoA
INS	Insulin
LDL	Low-density lipoprotein
LPO	Lipid hydroperoxide
MAFLD	Metabolic (dysfunction)-associated fatty liver disease
MTTP	Microsomal triglyceride transfer protein large subunit
NAFL	Non-alcoholic fatty liver
NAFLD	Non-alcoholic fatty liver disease

Abbreviation	Term
NAS	NAFLD activity score
NASH	Non-alcoholic steatohepatitis
NEFA	Non-esterified fatty acid
OVX	Ovariectomy/Ovariectomized
PEMT	Phosphatidylethanolamine N-methyltransferase
PL	Phospholipid
PNPLA3	Patatin-like phospholipase domain-containing protein 3
SAF	Steatosis, activity and fibrosis
SD	Sprague-Dawley
SDT	Spontaneously Diabetic Torii
SNPs	Single nucleotide polymorphisms
SREBP1	Sterol regulatory element-binding protein 1
SREBP2	Sterol regulatory element-binding protein 2
TC	Total cholesterol
TG	Triglycerides
VLDL	Very low-density lipoprotein

Chapter 1

General Introduction

Overview of the Liver Diseases

The liver is the largest organ in the human body and performs a variety of functions to maintain health. The liver plays three major roles: first, it synthesizes proteins from ingested nutrients to maintain the body and store nutrients; second, it detoxifies and breaks down substances that are harmful to the human body; and third, it synthesizes and secretes bile, which is necessary for the digestion of food. Thus, the liver is central to the production and circulation of nutrients. The liver can be seriously harmed by a variety of factors. Viral hepatitis, fatty liver disease, autoimmune conditions, genetic conditions, cirrhosis, and cancer are the major liver diseases.

Viral hepatitis is a liver disease caused by infection with hepatitis viruses, including types A, B, C, D, and E. Hepatitis A and E viruses are transmitted mainly through food, while hepatitis B, C, and D viruses are transmitted mainly through blood. Hepatitis B and C viruses, in particular, can cause chronic liver disease [1]. Symptoms such as fatigue, loss of appetite, nausea, and jaundice may occur, but often there are no symptoms at all. Diagnosis and treatment of viral hepatitis has evolved over the past several decades, with recent research aimed at curing and preventing the disease through drug therapy and liver transplantation.

Hepatic changes due to fatty liver disease include steatosis (accumulation of fat in hepatocytes) and steatosis-related liver damage. There are two types of fatty liver diseases: alcoholic and non-alcoholic. The former is clearly caused by heavy alcohol intake, but the factors and mechanisms underlying the development of non-alcoholic fatty liver disease (NAFLD) are not fully understood. Both types of fatty liver disease can

progress to cirrhosis and liver cancer via hepatitis if not managed. It has been reported that weight loss through diet, exercise, and lifestyle modification can improve the condition and greatly reduce the risk.

Several autoimmune diseases involve immune system attack on liver cells. Autoimmune hepatitis, primary cholestatic cholangitis, and primary sclerosing cholangitis are known, and all are designated intractable diseases in Japan. These diseases may lead to liver failure and cirrhosis [2–4].

Genetic factors can cause various liver pathologies including hereditary hemochromatosis, Gilbert syndrome, and Wilson disease. Because these diseases are hereditary, they are difficult to cure completely, but with appropriate therapeutic intervention, the prognosis is often good [5].

Cirrhosis refers to scarring caused by the diseases listed above or other factors that damage the liver. The liver can regenerate itself when damaged, and this process produces fibrosis in the liver. Chronic repeated damage and regeneration gradually leads to liver fibrosis and eventually to cirrhosis. Currently, there are still no effective strategies for treating cirrhosis. Part of the reason for this is that the molecular mechanisms leading to cirrhosis are not well understood [6].

As described above, liver diseases are diverse and, though asymptomatic in the early stage, can progress to cirrhosis and hepatocarcinoma with final fatal outcome. This fatal outcome is probably related to the fact that even when liver damage is present, subjective symptoms are rare and the progression of the disease is often overlooked. In addition, the liver plays a wide variety of roles in the body, and the cells that make up the liver are diverse. This is also an important medical feature, as the mechanisms of some diseases are not fully understood and appropriate treatment methods have not yet been established.

NAFLD/NASH

Among the liver diseases mentioned above, NAFLD and non-alcoholic steatohepatitis (NASH) have recently attracted worldwide attention. Schaffner *et al*. first used the name NAFLD in their 1986 review [7]. NAFLD is a metabolic syndrome of the liver and it is defined as the presence of steatosis of ≥5% of hepatocytes on histological or imaging diagnosis, after excluding other liver diseases such as alcoholic or viral diseases. The prevalence of NAFLD is estimated to be about 30% in the United States [8], and from 15 to 45% in Asia [9]. Thus, NAFLD has become a quite common liver disease worldwide and its increasing prevalence is alarming. NAFLD is histologically classified into non-alcoholic fatty liver (NAFL) and NASH. NASH is a more severe condition with necroinflammation, and it can progress to cirrhosis and hepatocellular carcinoma if left untreated. NASH accounts for 10-20% of all patients with NAFLD.

As with other complex diseases, genetic predisposition has a strong influence on the pathogenesis of NAFLD. Recent whole-genome studies have correlated up to one million single nucleotide polymorphisms (SNPs) with traits of NAFLD. Several studies reported the presence of multiple gene variants that correlate with the onset and susceptibility to progression of NAFLD. These variants are mutations in four genes: patatin-like phospholipase domain-containing protein 3 (PNPLA3), transmembrane 6 superfamily member 2, glucokinase regulator, and hydroxysteroid 17β-dehydrogenase [10–14]. PNPLA3 G/G genotype has been reported to correlate with the risk of NAFLD in normal-weight subjects. Twenty-five percent of the Japanese population has the G/G genotype, which may be one of the reasons why there are more non-obese NAFLD patients in Japan than in the West [15].

The first classification of NASH pathology was published by Matteoni *et al.* in 1999

[16]. In this classification, NAFLD was divided into four categories according to the presence of fatty degeneration of the liver, inflammatory cell infiltration of the liver parenchyma, ballooning degeneration of hepatocytes, Mallory-Denk bodies, and fibrosis. At the same time, NAFL and NASH were distinguished. However, the number of cases in this study was small, and later in 2011, their group proposed a new pathological classification [17]. In 1999, Brunt *et al*. proposed the Brunt classification of chronic hepatitis as applied to NASH [18]. This is based on the grading of fatty degeneration, ballooning degeneration, and inflammatory cell infiltration of the liver, and the staging of fibrosis. The NAFLD activity score (NAS) is used in the pathological diagnostic classification of all conditions of NAFLD based on the Brunt classification. An NAS of 5 or higher indicates NASH, a score of less than 3 indicates non-NASH, and a score in between indicates borderline NASH [19]. NAFLD activity scoring is used as a measure of NASH disease improvement in clinical drug development trials. The latest NASH pathology diagnostic criteria include the fatty liver inhibition of progression (FLIP) algorithm and the steatosis, activity and fibrosis (SAF) score to accompany the diagnosis. These were published in 2012 by Bedossa *et al*. [20]. In this algorithm, NASH starts with fatty degeneration and shows both ballooning degeneration of hepatocytes and inflammatory cell infiltration, while NAFLD does not show these characteristics. The SAF score is unique in that it separately describes steatosis and activity, which consist of ballooning degeneration and inflammatory cell infiltration, and includes fibrosis, which is not included in the FLIP algorithm. In a recent validation study, the FLIP algorithm and the SAF score are considered to be of high clinical relevance [21].

The mainstay of treatment for NAFLD/NASH is weight loss through caloric restriction and exercise. Weight loss is highly effective in improving NASH: a 5% reduction in body

weight is associated with improved quality of life, and a 7% or greater reduction in body weight is associated with histologic improvement. However, a 5% reduction in weight is achieved in only about 30% of patients, and the need for drug therapy is strongly recognized. Therefore, diabetes medications such as pioglitazone or antioxidants are sometimes used as background interventions, but their efficacy is limited [22].

Current Status of NASH Drug Development

The pipeline of NASH drugs currently in clinical development trials are remarkably diverse. They can be divided into three categories: glucose, lipid, and cholesterol metabolism modifiers; anti-inflammatory agents; and anti-fibrotic agents. The number of metabolism-ameliorating drug candidates with effects on NAFL as well as NASH is the largest in the NASH drug group. Obeticholic acid, which is considered to be the closest to approval, is also included here. Thus, despite the fact that many companies around the world have been trying to develop NASH drugs over the past decade, none have been approved. Several factors contribute to the difficulty of developing NASH treatment. First, NASH is a highly heterogeneous liver disease; NAFL in some patients with significant risk factors may not progress to NASH, and vice versa. In other words, progression to NASH may not be from the same cause or process in all patients. As a result, individual differences in response to drugs may be very large, and it may be difficult to evaluate the effects of drugs in a uniform manner. Second, clinical trials for NASH require a long time (more than one year), and an invasive and expensive liver biopsy is necessary to make a definitive diagnosis of the disease. The diagnosis by liver biopsy also does not exclude the possibility of variability among sample collection sites. The development of noninvasive, more accurate, and simpler markers of NASH pathophysiology is desired.

A final factor complicating the development of NASH therapeutics is the absence of animal models of the disease that accurately mimic the pathophysiology of human NASH patients. The existing animal models of NASH are discussed in detail in the next section. The development of drugs for the treatment of NASH is very challenging, but on the other hand very active due to the attractiveness of the market. However, many candidates, such as the anti-inflammatory drug Cenicriviroc (a C-C chemokine receptor type 2/5 antagonist), have been withdrawn from Phase III trials. In the future, combination therapies targeting multiple pathological mechanisms are expected to become primary NASH interventions [23].

Animal Models of NASH

Current animal models of NASH can be divided into three categories: genetic, dietary, and chemical administration models.

Known genetic models include leptin-deficient *ob/ob* mice, leptin receptor-deficient *db/db* mice, sterol regulatory element-binding protein 1 (SREBP1) c transgenic mice, acyl coenzyme A oxidase null mice, and KK-A^y mice [24–28]. The drawback of genetic models is that genetic mutations alone may not cause NASH. However, they are useful in examining the impact of specific signaling pathways on liver metabolism.

Dietary models are the most widely used and reported models because they are relatively similar to human NASH pathology and are less expensive to use. Typical diets used to create these models include a methionine choline deficient diet, a choline-deficient L-amino diet, a high-fat diet, a high-fructose diet, and a high cholesterol diet [29–32]. Feeding these diets to genetic models can also induce the development of NASH more efficiently.

Chemical administration models, such as the carbon tetrachloride (CCl_4) loading model, are characterized by the rapid and severe induction of NASH pathology, including fibrosis. Therefore, it is very useful for the evaluation of antifibrotic agents. On the other hand, the large burden of the drug often results in the death of animals during the administration period, and it is necessary to prepare a large number of animals to obtain stable results.

As mentioned earlier, the lack of a gold standard animal model of NASH pathology prevents the elucidation of the pathomechanisms of NASH. Also, unintentional use of "inappropriate" animal models may result in drugs that are successful in preclinical studies but not in clinical trials. Therefore, there is great interest in the development and validation of robust NASH pathology models that can be applied to human disease. Such a model would allow us to search for new target molecules that are strongly correlated with NASH progression. It would also allow us to validate a large number of candidate compounds and select those with high efficacy before entering clinical trials.

Purpose

The aim of this study was to develop novel NASH animal models. For this purpose, I evaluated NASH pathology in the liver of normal and type 2 diabetic rats by inducing metabolic abnormalities through surgical treatment or dietary challenge and investigated the mechanisms of the pathogenesis. In Chapter 2, I focus on the fact that male rodents are currently used in many existing NASH models, even though the risk of NASH is increased in elderly women. In my study, I used female Sprague-Dawley (SD) rats, Spontaneously Diabetic Torii (SDT) rats (a non-obese model of type 2 diabetes), and SDT fatty rats, which were transgenic for leptin receptor mutation (*Lepr*^{fa}) in SDT rats. Ovariectomies (OVX) were performed to deplete estrogen in each rat strain. Blood

biochemical values, liver lipid accumulation, liver fibrosis, and changes in liver genes expressions were examined. In Chapter 3, I note that female SD rats were fed a diet containing high cholesterol as a causative agent of NASH and cholic acid to promote its absorption. Although this diet has been used to produce pathology in existing NASH models, in this study some animals were given water containing hydroxypropyl-β-cyclodextrin (CDX) to enhance progression of the pathology and to improve usefulness in drug development. The effects of cholesterol overload on NASH pathological changes via cholesterol accumulation in the liver were evaluated, and the presence of oxidative stress and endoplasmic reticulum (ER) stress as underlying mechanisms was also examined. I will characterize each novel NASH model and discuss their advantages and disadvantages compared to existing NASH models and human patients.

Chapter 2

Establishment of a new non-alcoholic steatohepatitis model; Ovariectomy exacerbates nonalcoholic steatohepatitis-like pathology in diabetic rats

ABSTRACT

The number of patients diagnosed with NAFLD/NASH is increasing worldwide because of the growing prevalence of obesity and metabolic disorders. The incidence of NAFLD is higher in postmenopausal women than in premenopausal women. The decline in the level of female hormones might have an effect on the deterioration of metabolism.

In the present study, I investigated the potential of SDT-fatty rats as a new animal model for NAFLD. I created a menopausal model by OVX in female rats. SD rats, SDT rats, and SDT-fatty rats were divided into sham and OVX groups and maintained until 40 weeks of age. The results showed that OVX-induced weight gain was observed in SD and SDT rats. In addition, OVX-induced hepatic triglyceride accumulation was increased in all strains, and there was a significant increase in hepatic triglyceride levels in OVX-SDT fatty rats compared to those in sham-SD rats. Furthermore, liver fibrosis was worsened in the OVX-SDT fatty rats. In addition, OVX-induced increase in blood ALT level was observed in SDT-fatty rats. Gene expression analysis showed OVX-induced upregulation of *Srebp1* expression and downregulation of *Pemt* and *Mttp* in OVX rats. These results indicate that OVX-SDT fatty rats exhibit NASH with more severe hepatic fibrosis than untreated animals, suggesting that OVX-induced estrogen reduction may have enhanced lipid synthesis in the liver. It is also possible, although hypothetical, that OVX may decrease VLDL secretion, which may more strongly induce NASH.

INTRODUCTION

NAFLD is a chronic liver disease, which has been diagnosed in an increasing number of patients worldwide. NAFLD is a continuum of non-alcoholic liver dysfunction ranging from simple steatosis to NASH, and some of them progress to cirrhosis and liver cancer [33]. The majority of NAFLD patients have obesity, type 2 diabetes, and dyslipidemia; multiple factors (genetic, environmental, and epigenetic) are thought to influence disease development and progression, unlike in viral hepatitis and autoimmune liver diseases [34]. In recent years, in addition to these factors, age and sex differences have been considered factors responsible for the development of NAFLD. The prevalence and incidence of NAFLD tends to be higher in men than in premenopausal women (or those younger than 50–60 years), and higher in postmenopausal women (or those older than 50–60 years) [35]. This difference in the incidence and prevalence of NAFLD based on sex and age might be because of the presence of male hormones or female hormonal changes due to menopause. In fact, in young women with NAFLD, higher testosterone levels are associated with a higher risk of NASH and NASH-induced liver fibrosis, as well as a high risk of abdominal fat [36]. Furthermore, menopause is associated with changes in body composition, specifically with increased levels of intra-abdominal fat and increased waist circumference corrected for BMI, both of which are linked to an increased risk of metabolic diseases, including type 2 diabetes [37]. *In vitro* studies using human hepatocytes have shown that 17-β-estradiol inhibits cell death, mitochondrial dysfunction, and triglyceride accumulation under NAFLD-like conditions, suggesting that it has hepatoprotective effects [38]. In *in vivo*, non-obese male rats have decreased whole-body insulin sensitivity compared to female rats [39], and higher liver lipid accumulation when fed a high fat diet [40]. There have been many reports on the influence of sex hormone

differences on metabolic diseases [41,42], and as mentioned above, the same possibility has been suggested for NAFLD/NASH. There is evidence of protective effects of female hormones on hepatocytes and liver tissue at the *in vitro* and *in vivo* levels, which is consistent with the fact that the incidence of NASH in women increases after menopause.

The etiology and pathogenesis of NAFLD/NASH are complex, and not all of them are clear. Although the gold standard for NASH animal models has not yet been established, a variety of models exist.

The SDT-fatty rat is a type 2 diabetes model in which a leptin receptor mutation is introduced into the genetic background of SDT rats. This mutation is an obesity gene in Zucker fatty rats. SDT-fatty rats show obesity, hyperglycemia, and hyperinsulinemia due to polyphagia at a young age [43], and female SDT-fatty rats show NASH-like symptoms at a high age without food loading [44]. Since many human patients with NAFLD are also obese and have type 2 diabetes mellitus [45], I hypothesized that this model would be useful for studying the pathogenesis of NAFLD in humans. The ovariectomized (OVX) animal model is a postmenopausal female model that allows for NAFLD-like pathogenesis, such as steatosis and liver damage [46,47]. The main objective of this study was to investigate the possibility of using OVX-SDT fatty rats as a new NASH model by assessing the pathogenesis of NAFLD. For this purpose, I determined the pathological changes in the liver after OVX, measured the body weight, blood biochemical values, and lipid content of the liver, and evaluated the expression of lipid synthesis and fibrosis-related genes in the liver. OVX was also applied to SD rats as normal controls and SDT-fatty rats as genetic background controls, and various evaluations in the liver were performed.

MATERIALS AND METHODS

Animals

Female SD rats, female SDT fatty rats, and female SDT rats were purchased from CLEA Japan Inc. (Tokyo, Japan). At 6 weeks of age, each rat lineage was divided into two groups (n = 5): a sham group and an OVX group. The animals were housed in a room climate-controlled for temperature (23 ± 3°C), humidity (55 ± 15%), and lighting (a 12 h dark-light cycle). All animals were fed a normal diet (CRF-1, Oriental Yeast Co., Ltd., Tokyo, Japan) and had free access to water. One animal in the SD rat sham group died during the experimental period, bringing the total number of animals in this group to n = 4. All remaining animals were necropsied at 40 weeks of age. All experimental protocols and animals were used according to strict compliance with our own laboratory guidelines for animal experimentation.

Tissue sampling and histopathological evaluation

Dissections were performed at 40 weeks of age. Animals were sacrificed by exsanguination under isoflurane anesthesia. The livers were sampled for determining the hepatic lipid content and analysis of mRNA expression and histopathology. The samples for liver lipid mass and mRNA analysis were frozen at -80°C until use. For pathological analysis, the livers were fixed in 10% neutral buffered formalin immediately after collection. The tissues were paraffin-embedded by standard techniques and thin-sectioned (3 to 5 μm). For histopathological evaluation and liver fibrosis analysis, tissue sections were H&E stained and Sirius Red stained, respectively. The Sirius Red-positive area ratio was used as a liver fibrosis marker. Immunohistochemical examinations were conducted using antibodies against CD44 (Cell Signaling Technology, Inc., Danvers, MA, USA).

Histofine Simple Stain Rat MAX-PO (MULTI) (Nichirei Bioscience Inc., Tokyo, Japan) was used as a secondary antibody, and the signals were visualized using 3,3′-diaminobenzidine (Wako Pure Chemical Industries, Ltd., Osaka, Japan).

Hepatic lipid contents

Approximately 100 mg of liver sections were taken in tubes, and zirconia beads and methanol (0.5 mL) were added. The samples were homogenized using a mixer mill (MM300 Retsch, Haan, Germany) (25 Hz, 10 min). To extract lipids from the homogenized solution, 1 mL of chloroform was added and mixed. All samples were then centrifuged (10,000 × *g*, 5 min, 4°C) and the supernatant (0.5 mL) was collected in other tubes and dried with nitrogen gas. The residue was dissolved in 0.5 mL 2-propanol. The TG, TC, and PL concentrations of the sample solutions were measured as fatty liver-related markers using a biochemistry automatic analyzer (Hitachi 7170S; Hitachi, Tokyo, Japan).

mRNA quantification

Total RNA was extracted from approximately 20 mg liver sections using the GenElute™ Mammalian Total RNA Miniprep Kit (MilliporeSigma, Burlington, Massachusetts, USA) according to the manufacturer's protocols. Reverse transcription was performed using the High-Capacity cDNA Reverse Transcription Kit with an RNase Inhibitor (Applied Biosystems, Foster City, California, USA) to synthesize complementary DNA (cDNA) from 1 μg of total RNA. For reverse transcription, the reaction mixture was incubated at 25°C for 10 min, 37°C for 120 min, and 85°C for 5 min. Gene expression was quantified using TaqMan Gene Expression Assays: Liver lipid-

related genes: *Fasn* (Rn00569117_m1), *Scd1* (Rn06152614_s1), *Srebp1* (Rn01495769_m1), *Pemt* (Rn00564517_m1), *Mttp* (Rn01522963_m1); Fibrosis-related genes: *Col1a1* (Rn01463848_m1), *Acta2* (Rn01759928_g1), *Tgfb1* (Rn99999016_m1); Endogenous control gene: *Gapdh* (Rn99999916_s1). Real-time PCR was performed in a 10 μL reaction mixture contained 10 ng of cDNA with QuantStudio 7 Flex (Thermo Fisher Scientific, Waltham, Massachusetts, USA). The cycle parameters included 10 min at 95°C followed by 40 cycles of 15 sec at 95°C and 60 sec at 60°C. The mRNA levels were calculated using *Gapdh* as the reference gene, and the expression levels in each group were corrected by the mean of the SD sham group.

Biological parameters

Body weight was measured at 6, 8, 16, 24, 32, and 40 weeks of age. Blood samples were collected from the rat tail vein at the beginning of the study and before autopsy to measure the following blood biochemical parameters: glucose (GLU), insulin (INS), triglycerides (TG), total cholesterol (TC), phospholipid (PL), alanine aminotransferase (ALT), and aspartate aminotransferase (AST). GLU, TG, TC, PL, ALT, and AST levels were measured using respective product kits (Roche Diagnostics, Tokyo, Japan) and an automatic analyzer (Hitachi). INS levels were measured using enzyme-linked immunosorbent assay kits (Morinaga Institute of Biological Science, Yokohama, Japan).

Statistical analysis

All values are expressed as the mean ± standard deviation. Statistical analyses between groups were performed as follows: Student's t-test or Aspin-Welch’s t-test was used to compare the means of the two groups. In the comparison of multiple groups, Bartlett's

test was first used to test for equal variability among the groups. As a result of the Bartlett test, Dunnett's test was used if data followed homoscedasticity, and Kruskal-Wallis test, followed by Dunn's multiple comparisons test, was used as a nonparametric test method if samples had no equal variances. The criterion for a significant difference was set at $P < 0.05$.

RESULTS

Weight change after OVX

OVX-induced obesity was observed in SD and SDT rats; SD rats showed significant weight gain compared to sham from 16 weeks of age (10 weeks after OVX), which continued until autopsy (Fig. 1A), and SDT rats showed significant weight gain from 2 to 10 weeks after OVX. The body weight of the OVX group remained higher than that of the sham group until autopsy (no significant difference) (Fig. 1B). In contrast, SDT-fatty rats were more obese than SD and SDT rats throughout the study period, but no OVX-induced weight gain was observed in the same strain (Fig. 1C). This suggests that OVX-induced weight gain may be difficult to detect in SDT-fatty rats because they are extremely obese under normal conditions.

Effects of OVX on liver weight and hepatic lipids

The liver weight per body weight of SDT-fatty rats tended to be greater than that of SD and SDT rats in the same treatment. In contrast, no increase in liver weight was observed in either strain of OVX rats (Fig. 2A). To evaluate lipid accumulation in the liver, hepatic TG, TC, and PL contents were measured in the liver sections. The liver TG content was

markedly increased, and PL content was considerably decreased in the OVX group of SDT-fatty rats compared to that in the sham group of SD rats (Fig. 2B–D).

Changes in blood biochemistry values by OVX

The blood GLU, INS, TG, TC, and PL levels of SDT-fatty rats were significantly higher than those of SD rats at the beginning of the study, suggesting that they developed diabetes and abnormal lipid metabolism (Fig. 3A-D, G). AST and ALT levels, indicative of liver damage, were also significantly higher (Fig. 3E, F). No abnormalities were observed in the blood biochemical parameters of SDT rats of the same age, suggesting that they did not develop diabetes at the beginning of the study. Blood chemistry values at necropsy showed significantly higher levels of TG, TC, and PL in both sham and OVX rats compared to those of the sham group of SD rats (Fig. 3B–D). There was also a significant increase in ALT levels in the SDT-fatty OVX group (Fig. 3E). Blood AST levels showed an increasing trend in the SDT-fatty OVX group (Fig. 3F). A significant increase in blood INS levels was observed only in the sham group of SDT rats compared to those in SD rats (Fig. 3G). As an effect of OVX in SDT-fatty rats, blood TG, TC, and PL tended to decrease (though not significantly different).

Liver histopathologic evaluation

Microphotographs of liver tissue with H&E stain are shown in Fig. 4A. Fatty liver and hypertrophy of hepatocyte in SDT-fatty rats tended to be exacerbated by OVX (Table 1). As inflammation marker of liver, CD44 immunostaining was performed; however, inflammation was largely unaffected by OVX (Fig. 4B and Table 1). Liver fibrosis is an important index for assessing the disease prognosis in patients with NASH. Liver fibrosis

was assessed by liver sections stained with Sirius Red (Fig. 4C). There was a significant increase in the area of hepatic fibrosis in OVX SDT-fatty and SDT rats compared to that in sham rats. However, this change was not observed in OVX SD rats (Fig. 4D). In histopathological imaging, OVX of SDT-fatty rats showed fibrous extension from the central venous region of the lobules to the surrounding tissues, and OVX of SDT rats showed Sirius Red-positive areas in the tissues, whereas in SD rats, these changes were hardly observed in OVX rats (Fig. 4C). OVX-induced liver fibrosis was found to be progressive in an animal model with a diabetic background.

Effects of OVX on liver gene expression

The mRNA levels of lipid-related genes (*Fasn*, *Scd1*, *Srebp1*, *Pemt*, and *Mttp*) and fibrosis-related genes (*Col1a1*, *Acta2*, and *Tgfb1*) in the liver were measured using real-time PCR (Fig. 5). Compared with that in the SD sham rats, *Srebp1*, a lipid synthesis gene, was upregulated approximately two-fold in OVX of SDT fatty rats (Fig. 5C), and the expression of *Pemt*, a major PL synthase in the liver, and *Mttp*, which is involved in the secretion of very low-density lipoprotein (VLDL), was significantly decreased (Fig. 5D–E). In contrast, there was no change in the expression of fibrosis-related genes (Fig. 5F–H). *Fasn* and *Srebp1* mRNA expression was significantly upregulated in OVX SDT rats compared with SD sham rats, and *Scd1* also showed an increasing trend ($P = 0.0626$) (Fig. 5A–C), while *Pemt* and *Mttp* mRNA levels were unchanged (Fig. 5D–E). These results showed that there was a difference in the profile of OVX-induced hepatic gene expression between SDT-fatty rats and SDT rats.

DISCUSSION

NAFLD/NASH is a liver disease that has attracted increasing attention because of the recent increase in the number of patients worldwide. It is a major cause of hepatocellular carcinoma, and many animal models for studying its pathogenesis have been reported. There are three main types of animal models for NASH: dietary burden models, genetically modified models, and drug-induced models. Typical models of each type include the choline-deficient L-amino-defined (CDAA) diet model, *db/db* mice, and CCl_4 model, respectively. The CDAA dietary model is a useful model for drug evaluation because it shows extreme fatty liver and inflammation, and rapid pathogenesis of liver fibrosis and hepatocarcinoma [31]. However, this model does not show weight gain or insulin resistance [48,49], and is considered to have a different metabolic profile from human NASH, making it an incomplete surrogate model for human disease. *db/db* mice are deficient in leptin signaling owing to mutations in the leptin receptor gene, and spontaneously develop typical NAFLD-like pathology, including overeating, obesity, insulin resistance, and fatty liver [50]. However, additional stimulation with a high-fat diet or a methionine-choline-deficient diet is required to show the features of NASH. The ability of this model to lead to advanced fibrosis and hepatocellular carcinoma has not been adequately investigated. Repeated administration of CCl_4 has become one of the most common approaches to create models of drug-induced liver fibrosis, and long-term oral administration of CCl_4 results in significant hepatotoxicity with liver fibrosis, cirrhosis, and hepatocellular carcinoma [51]. This feature of CCl_4 is used for the evaluation of anti-fibrotic drugs, but its use is limited by the fact that it does not exhibit obesity and deviates from human NASH pathology, and deaths occur with long-term administration. As described above, each animal model of NASH has its own advantages

and disadvantages, and there is currently no model that can completely mimic human NASH.

In a previous study, SDT-fatty rats developed metabolic abnormalities including hyperglycemia and hyperinsulinemia at a young age, and there was no difference in the pathogenesis between males and females [52], but the pathophysiological features of NASH with fibrosis were only observed in female SDT-fatty rats [44]. In the present study, I showed that OVX-induced deterioration of lipid metabolism and the resulting worsening of NASH pathology were observed through the measurement of blood biochemical values and lipid content in the liver, gene expression analysis, and fibrosis analysis of liver tissue. OVX SDT-fatty rats showed elevated liver TG content, elevated ALT, a marker of liver injury, and increased liver fibrosis area, which were significantly different from those of SD sham rats. I focused on the reduction of lipid secretion from the liver as a mechanism of OVX-induced TG accumulation in the liver.

OVX in SDT-fatty rats showed a tendency to decrease blood TG, TC, and PL, which are components of VLDL secreted by the liver, at autopsy compared to sham rats [53]. PEMT plays an important role in PL biosynthesis in the liver. An OVX-induced decrease in *Pemt* was observed in SDT-fatty rats, and a downward trend was also observed in other rat strains. In *in vitro*, mRNA expression and enzymatic activity of PEMT are upregulated by 17β-estradiol stimulation [54], and in vivo, NASH models lacking PEMT have been reported to have a worse condition compared to wild-type [55]. In SDT-fatty rats, PL synthesis in the liver might be suppressed by the OVX-induced reduction of female hormone levels. In addition, *Mttp* mRNA levels were decreased in both sham and OVX rats of SDT-fatty rats compared to those in sham of SD rats. Microsomal triglyceride transfer protein large subunit (MTTP) is involved in VLDL secretion from the liver and

is downregulated by OVX in rats; additionally, it has been reported that estrogen supplementation restores *Mttp* mRNA expression in these animals [56]. In other words, the synthesis of PL, the substance of VLDL, is suppressed in OVX of SDT-fatty rats, and lipid accumulation in the liver might be aggravated by the suppression of VLDL secretion due to the decrease in MTTP.

An important feature of NASH pathology is inflammation of the liver as well as steatosis. In many studies of animal models of NASH, evaluation of liver pathology and elevated inflammatory cytokines have confirmed the establishment of NASH pathology. In this study, we evaluated liver inflammation and found no effect of OVX on mRNA expression of pro-inflammatory cytokines or inflammatory cell infiltration into the liver. Liver fibrosis is an important prognostic indicator in NASH, and in this study, I observed increased liver fibrosis area in OVX SDT-fatty rats, but no elevation of fibrosis-related genes. Previous studies have shown that these inflammation- and fibrosis- related genes are not altered in female SDT-fatty rats at 40 weeks of age and are upregulated at earlier time points [44]. It is probable that hepatic inflammation and fibrosis developed before 40 weeks of age in the present study, and the secretion of pro-inflammatory cytokines and activation of fibrosis-promoting reaction were reduced as the disease progressed. This study focused on capturing the pathological changes of liver fibrosis as the most important feature of NASH pathogenesis, and long-term rearing was conducted. On the other hand, earlier observation may be necessary to capture inflammatory pathology and the expression of NASH-related genes in the liver. The timing of observation is critical for the use of this model, and further research is needed to determine the time point at which all NASH characteristics can be captured simultaneously.

OVX-induced increase in liver fibrosis area was also observed in SDT rats, the genetic

background of SDT-fatty rats. In a previous study, female SDT rats showed only fatty liver histopathology at 40 weeks of age [57] and no liver fibrosis. Therefore, it is possible that the worsening of metabolic abnormalities caused by OVX affected the development of hepatic fibrosis. However, unlike SDT-fatty rats, SDT rats did not show OVX-induced changes in parameters characteristic of NASH, such as increased lipids in the liver and elevated blood ALT and AST levels at 40 weeks of age.

In the blood biochemistry at the beginning of the study, SDT rats showed slightly higher ALT and AST levels than SD rats, but not as high as SDT-fatty rats. The blood GLU, TG, and INS levels were similar to those of SD rats. Gene expression in the liver showed that *Fasn* and *Srebp1* were strongly expressed in SDT rats compared to those in SDT-fatty rats, and the mRNA expression of the inflammatory cytokines *Tnf* and *Ccl2* was upregulated (data not shown). These characteristics suggest that the process of OVX-induced disease progression in SDT rats may be considerably different from that in SDT-fatty rats. Further studies are needed to elucidate the mechanism of OVX-induced liver fibrosis in SDT rats.

In conclusion, female SDT and SDT-fatty rats showed liver fibrosis with fatty liver at 40 weeks of age after OVX. Female SDT-fatty rats show NASH pathophysiology without any special treatment, but OVX further develops this pathology, suggesting that it may be an important NASH model.

Table 1 Histopathological findings in liver

	SD Sham				SD OVX					SDT Sham					SDT OVX					SDT-fatty Sham					SDT-fatty OVX				
	1	2	3	4	1	2	3	4	5	1	2	3	4	5	1	2	3	4	5	1	2	3	4	5	1	2	3	4	5
Hepatosteatosis (Vacuolation/Fatty change)	–	–	–	–	–	±	±	–	–	±	±	–	±	±	±	±	+	±	–	±	±	–	±	+	2+	+	+	–	+
Hypertrophy of hepatocyte	–	–	–	–	–	–	–	–	–	±	–	–	–	±	±	–	+	±	–	–	–	–	±	+	+	+	+	–	+
Infiltration, inflammatory cells	–	–	–	–	–	–	±	±	–	±	–	–	–	–	–	–	–	–	–	–	±	–	–	–	–	–	–	–	±
Fibrosis	–	–	–	–	–	–	–	–	–	±	–	–	–	–	+	±	±	–	–	±	±	±	±	±	+	+	+	–	±

–; Negative, ±; Very slight, +; Slight, 2+; Moderate, 3+; Severe

Summary of pathological evaluation by H&E staining (hepatosteatosis and hypertrophy of hepatocyte), CD44 immunostaining (infiltration of inflammatory cells), and Sirius Red staining (fibrosis) are represented (n = 4–5).

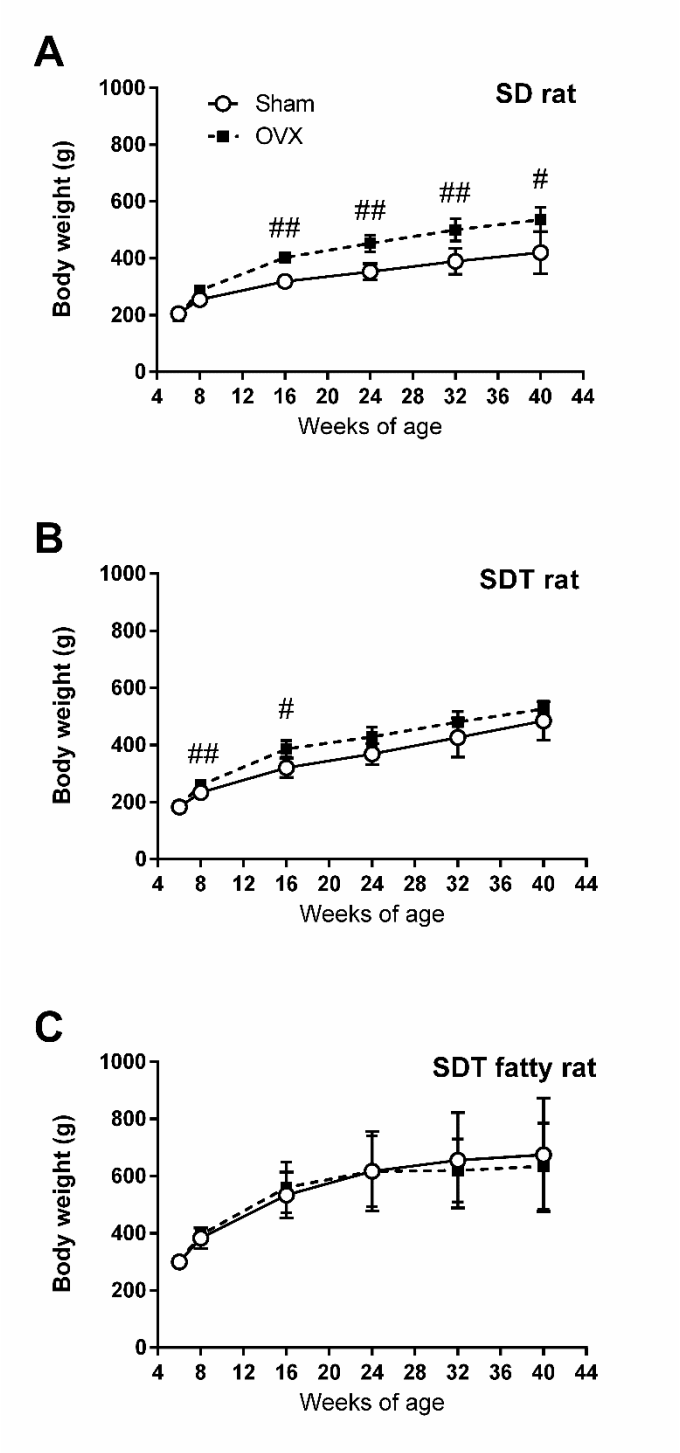

Fig. 1 Changes in body weight in SD, SDT, and SDT-fatty rats

(A) SD rats, (B) SDT rats, (C) SDT-fatty rats

Data are shown as mean ± standard deviation ($n = 4–5$). #$P < 0.05$, ##$P < 0.01$,

comparison with sham of each strain.

SD: Sprague-Dawley, SDT: Spontaneously diabetic Torii, SDT-fatty: Spontaneously diabetic Torii fatty, OVX: Ovariectomized

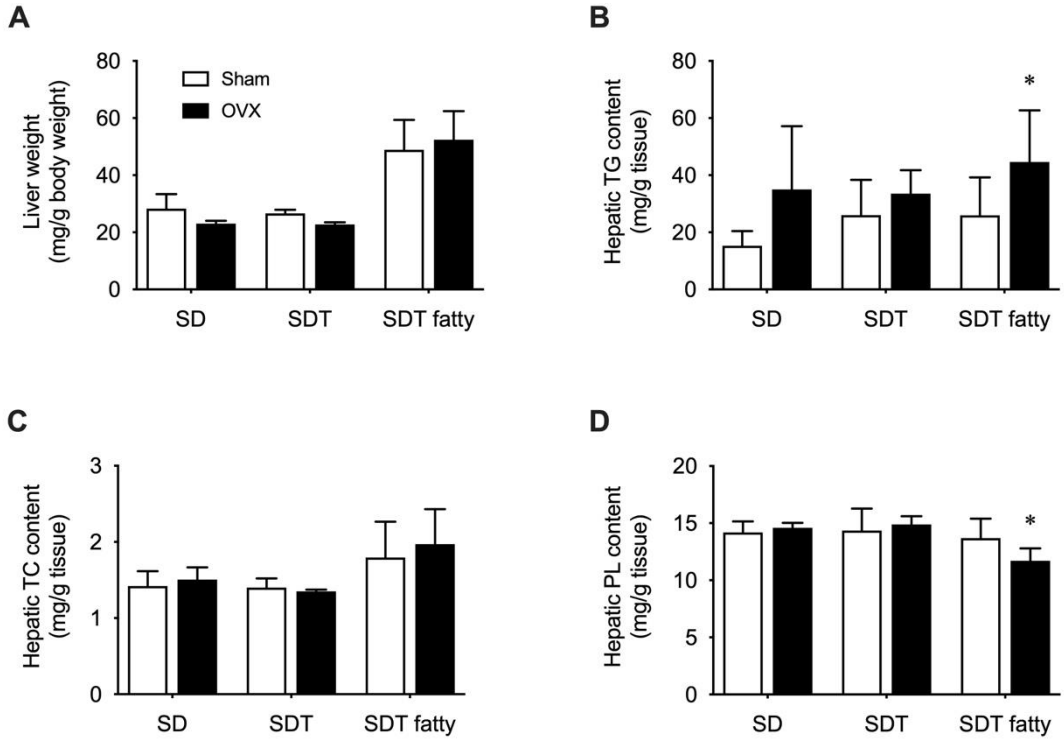

Fig. 2 Liver weight and liver lipid contents at 40 weeks of age in SD, SDT, and SDT-fatty rats

(A) Liver weight (mg) per g body weight, (B) Liver TG, (C) Liver TC, (D) Liver PL

Data are shown as mean ± standard deviation (n = 4–5). *P < 0.05, comparison with sham of SD rats.

TG: Triglyceride, TC: Total cholesterol, PL: Phospholipids

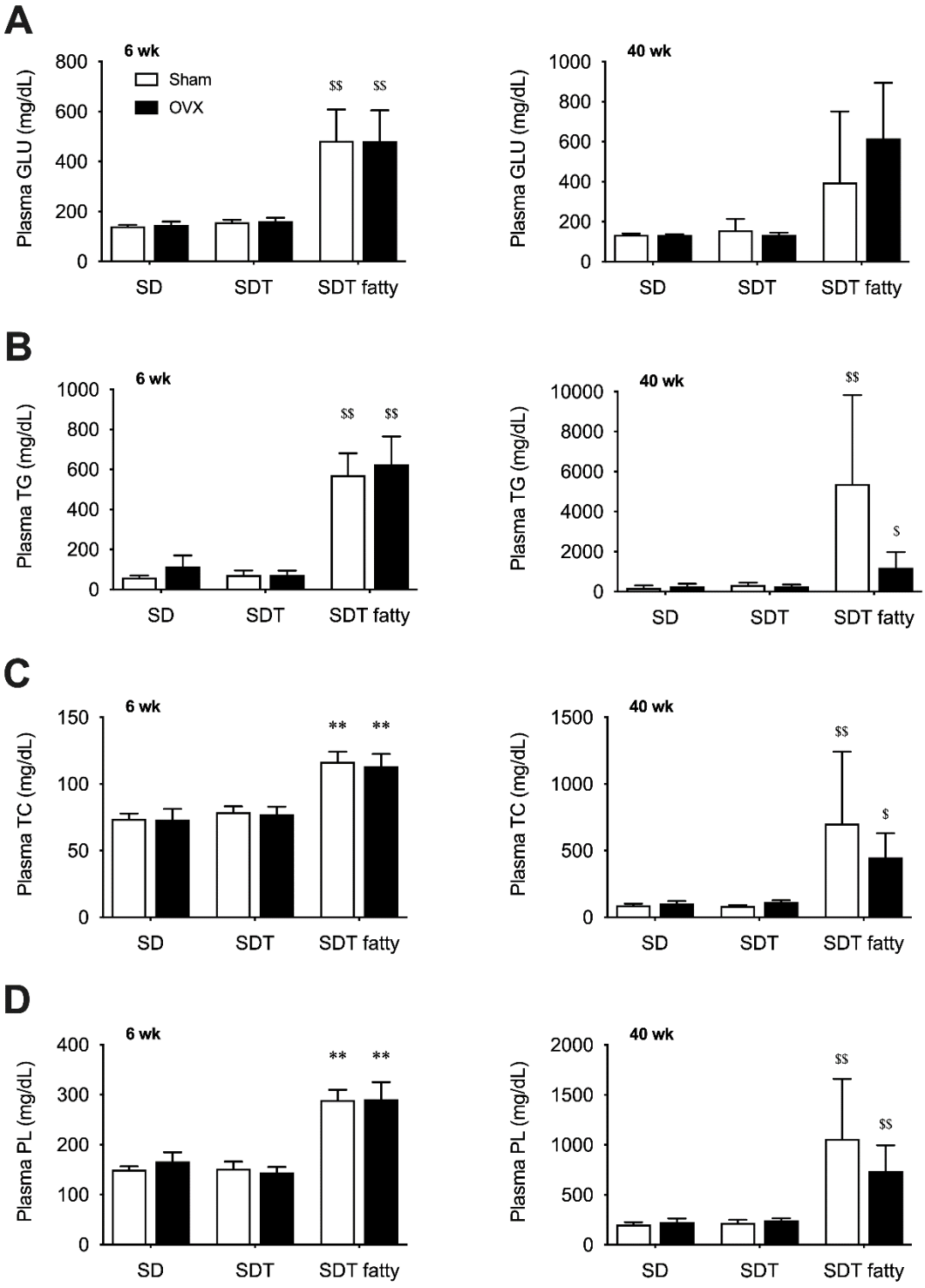
A
6 wk
Sham
OVX
Plasma GLU (mg/dL)
800
600
400
200
0
$$
$$
SD
SDT
SDT fatty
40 wk
1000
800
600
400
200
0
B
6 wk
Plasma TG (mg/dL)
1000
800
600
400
200
0
40 wk
10000
8000
6000
4000
2000
$
C
6 wk
Plasma TC (mg/dL)
150
100
50
**
**
40 wk
1500
1000
500
D
6 wk
Plasma PL (mg/dL)
400
300
200
100
40 wk
2000
1500
1000
500

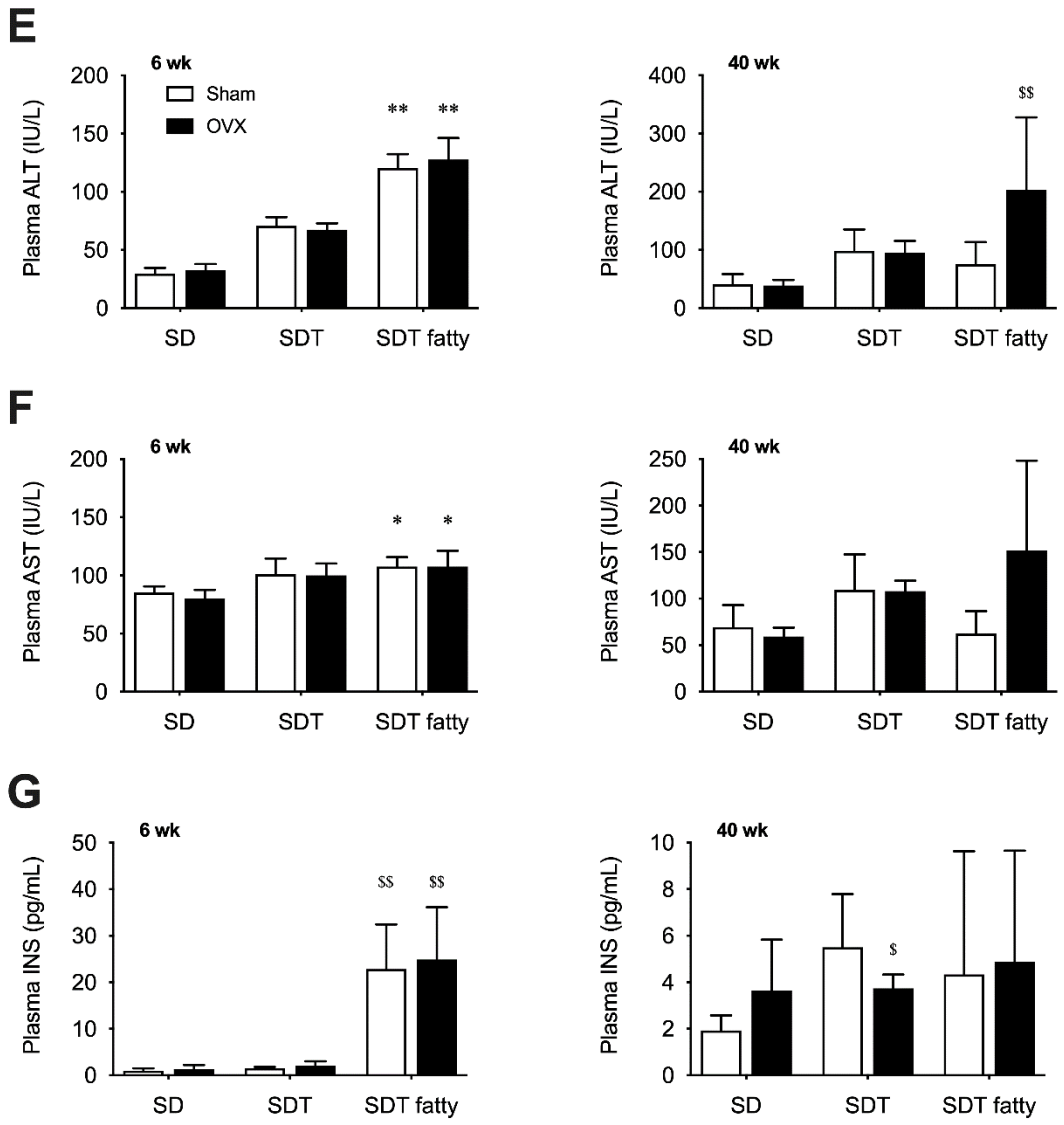

Fig. 3 Blood biochemical values at the beginning and the end of the study in SD, SDT, and SDT-fatty rats

(A) Plasma GLU, (B) Plasma TG, (C) Plasma TC, (D) Plasma PL, (E) Plasma ALT, (F) Plasma AST, (G) Plasma INS

Left panel: pre (6 weeks of age), Right panel: post (40 weeks of age)

Data are shown as mean ± standard deviation (n = 4-5). *$P < 0.05$, *$P < 0.01$ Dunnett's multiple comparison with sham of SD rats. \$$P < 0.05$, \$\$$P < 0.01$ Dunn's multiple comparison with sham of SD rats.

GLU: Glucose, TG: Triglyceride, TC: Total cholesterol, PL: Phospholipids,

ALT: Alanine transaminase, AST: Aspartate transaminase, INS: Insulin

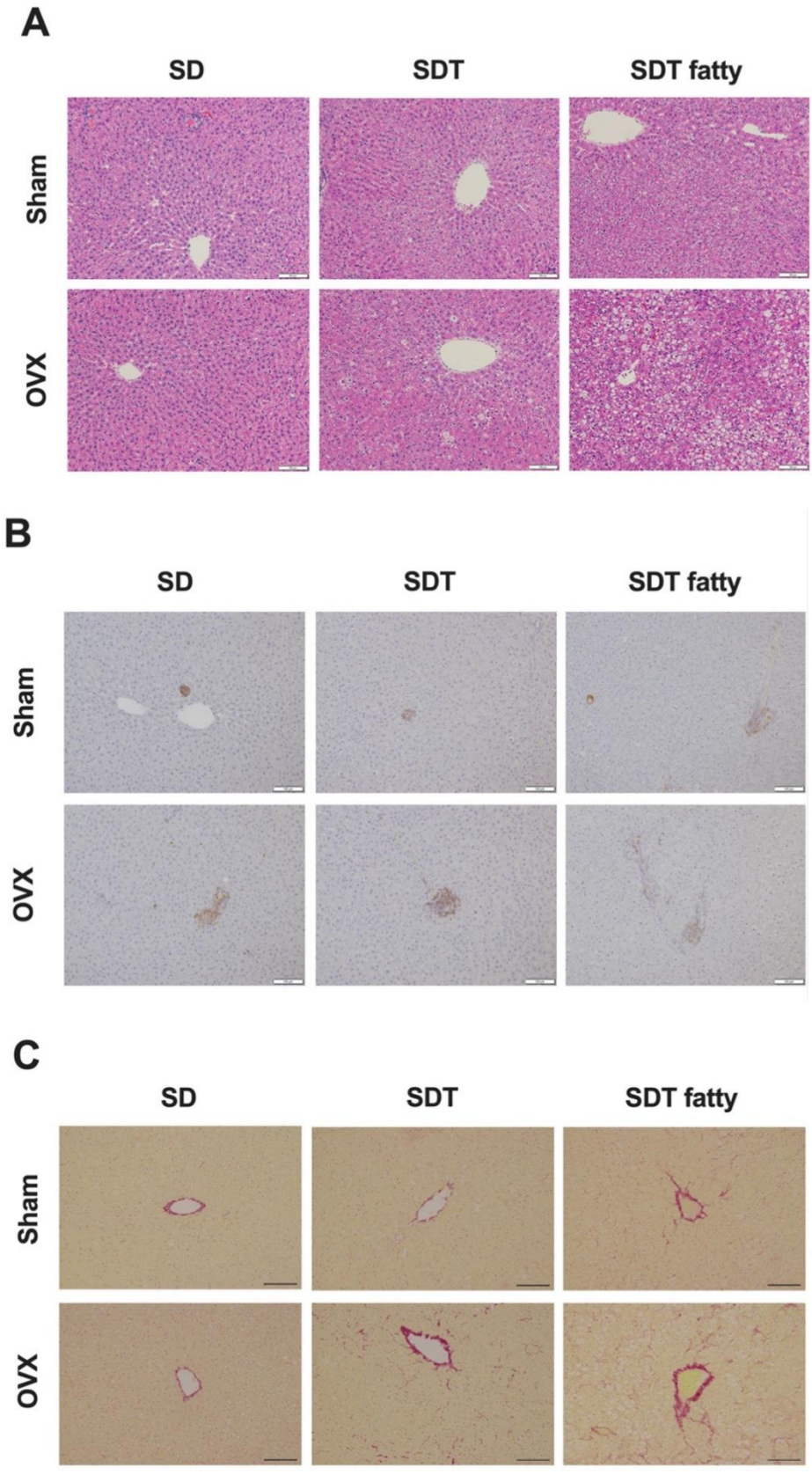
A
SD
SDT
SDT fatty
Sham
OVX
B
SD
SDT
SDT fatty
Sham
OVX
C
SD
SDT
SDT fatty
Sham
OVX

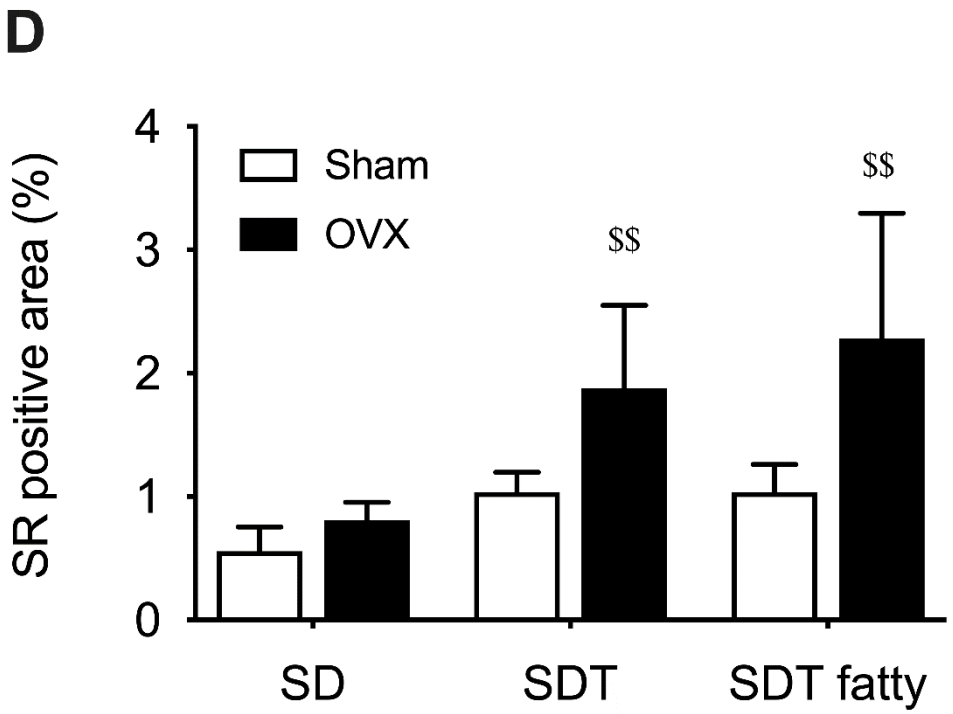

Fig. 4 Histopathological changes in SD, SDT, and SDT-fatty rats at 40 weeks of age

Representative pictures of stained specimens from each group of animals are shown.

(A) H&E staining of liver sections. Scale bars: 100 μm. (B) CD44 immunostaining of liver sections. Scale bars: 100 μm. (C) Sirius Red staining of liver sections. Scale bars:100 μm, (D) Sirius Red-positive area (%). Data are shown as mean ± standard deviation (n = 4–5). \$\$$P < 0.01$, Dunn's multiple comparison with sham of SD rats.

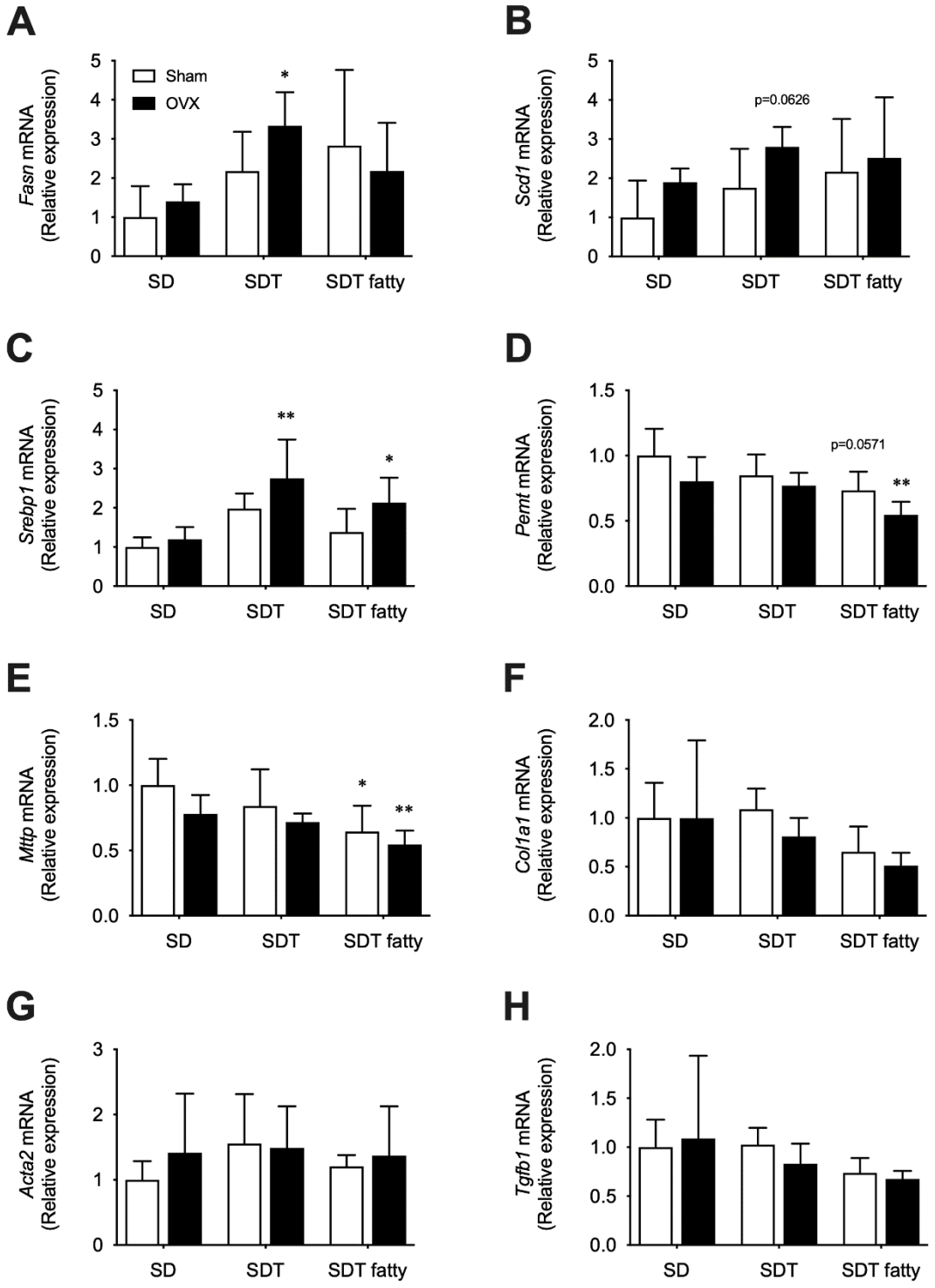

Fig. 5 Expression of hepatic genes related to lipid synthesis, lipid secretion and fibrosis at 40 weeks of age of SD, SDT, and SDT-fatty rats

(A) *Fasn*, (B) *Scd1*, (C) *Srebp1*, (D) *Pemt*, (E) *Mttp*, (F) *Col1a1*, (G) *Acta2*, (H) *Tgfb1*

Data are shown as mean ± standard deviation (n = 4–5). *P < 0.05, **P < 0.01 Dunnett's multiple comparison with sham of SD rats.

Chapter 3

Development of a novel rat model of non-alcoholic steatohepatitis in which cholesterol and hydroxypropyl-β-cyclodextrin loading induces pathogenesis

ABSTRACT

NAFLD is a general term for fatty liver disease not caused by viruses or alcohol. Fibrotic hepatitis, cirrhosis, and hepatocellular carcinoma can develop. The recent increase in NAFLD incidence worldwide has stimulated drug development efforts. However, there is still no approved treatment. This is partly due to the lack of a standardized animal model that mimics the pathogenesis of human NAFLD, including NASH. Due to the close association between the establishment of human NAFLD/NASH pathology and metabolic syndrome, several animal models have been reported, especially in the context of overnutrition. In this study, I attempted to create a new NAFLD/NASH model using SD rat cholesterol overload and its enhanced absorption by treatment with CDX. Rats were fed a normal diet with normal water (control group); a high-fat (60 kcal%), cholesterol (1.25%), and cholic acid (0.5%) diet with normal water (HFCC group); or HFCC diet with 2% CDX water (HFCC+CDX group) for 16 weeks. Compared to the control group, the HFCC and HFCC+CDX groups showed increased blood levels of TC, AST, and ALT, 8 weeks after the start of loading. At autopsy, parameters related to hepatic lipid synthesis, oxidative stress, inflammation, and fibrosis were elevated, suggesting the development of NAFLD/NASH. Elevated levels of ER stress-related genes were evident in the HFCC+CDX group. In the novel rat model, excessive cholesterol intake and accelerated absorption contributed to NAFLD/NASH pathogenesis.

INTRODUCTION

NAFLD is a general term for chronic liver disease in which a fatty liver is present and there are no other causes of liver injury, including alcoholic or viral liver disease [33,58]. The accumulation of triglycerides in the liver is a relatively benign condition and is the result of a mechanism that protects the liver by converting incoming harmful fatty acids such as saturated free fatty acids into relatively safe forms. However, in some fatty liver patients, the condition progresses to NASH, which is characterized by persistent hepatitis, tissue damage, and liver fibrosis [33]. In particular, liver fibrosis correlates most strongly with prognosis and mortality in NASH patients because it can progress to cirrhosis and hepatocarcinoma [59]. The prevalence of NAFLD and NASH continues to increase and has reached 30% and 12%, respectively, in the United States [8]. Liver disease due to NASH is predicted to become a major cause of liver transplantation [60]. Accordingly, drug development for NAFLD/NASH has become a research priority. Clinical trials are underway for many candidate compounds. While a drug treatment for NAFLD/NASH will likely be available in the near future, no approved treatment presently exists. Factors hindering drug development include the complex and poorly understood mechanisms of NAFLD/NASH pathogenesis, a very heterogeneous liver disease that is unlikely to respond to a single-drug approach, and the lack of a gold standard animal model.

The etiology of the progression from simple fatty liver to NASH remains unclear. The "two-hit hypothesis" proposed that the first hit, hepatic steatosis, is followed by a second hit, stress, which causes inflammation and liver injury. The latter lead to the progression to NASH. This hypothesis does not adequately explain some of the molecular and metabolic changes that occur in NAFLD and is now considered outdated. The "multiple-hit hypothesis" proposes that NASH is induced by the addition of multiple factors in

genetically predisposed patients [61,62]. These factors include insulin resistance, hormones, and gut microbiota. In recent years, metabolic (dysfunction)-associated fatty liver disease (MAFLD) has been proposed, considering its close association with metabolic abnormalities [63,64]. In fact, NAFLD is frequently complicated by various dysmetabolic diseases, such as obesity, type 2 diabetes, hyperlipidemia, and chronic kidney disease [65–70].

An ideal animal model would mimic the pathophysiology of NASH in humans. It should have the typical features of NASH, such as obesity, liver fat deposition, inflammation, and ballooning. For drug development, it is also important to assess liver fibrosis, which is highly correlated with NASH prognosis. Animal models of NASH used in non-clinical settings can be classified into three categories: dietary burden, genetically modified, and drug-induced models [71]. Dietary burden models are frequently used because of their simplicity. However, their drawback is that long-term dietary challenges are required for the development of NASH pathophysiology.

In the context of NAFLD/NASH, I focused on the possibility of animal models of NASH caused by the hepatic accumulation of cholesterol as the cause of metabolic abnormalities. Liver is important in cholesterol homeostasis. Similar to triglycerides, cholesterol esters are a relatively safe form of lipid storage. However, accumulation of free cholesterol in the liver is highly toxic to multiple intracellular processes and organelles [72]. Although there are many cholesterol-loaded NASH models, a model of very early onset of NASH pathology has recently been reported in mice fed a high-fat, high-cholesterol, and cholic acid-containing diet with CDX water [73,74]. In these reports, CDX water was used to increase cholesterol absorption.

I evaluated the potential of cholesterol overload and its absorption enhancement in SD

rats as a new NAFLD/NASH model. I measured liver steatosis, inflammation, and fibrosis-related parameters in response to high-fat and cholesterol loads and determined the pathogenesis of NASH pathology in the rats. In addition, I investigated oxidative stress and ER stress in the liver.

MATERIALS AND METHODS

Animals

Four-week-old female SD rats were purchased from CLEA Japan and acclimatized for 2 weeks. The animals were housed in a room climate-controlled for temperature (23±3°C), humidity (55±15%), and lighting (12 h dark-light cycle). At 6 weeks of age, the animals were divided into three groups (n=6 per group) with equal mean values for body weight, blood AST, ALT, and total TC levels. During the experimental period, each group of animals was fed a normal diet (CRF-1) with normal water (control group); high-fat (60 kcal%), cholesterol (1.25%), and cholic acid (0.5%) diet (HFCC; D11061901, Research Diets, New Brunswick, New Jersey, USA) with normal water (HFCC group); or HFCC diet with 2% CDX water (HFCC+CDX group). The animals were dissected at 22 weeks of age and liver samples were collected. All animals were handled in strict compliance with the laboratory guidelines for animal experimentation set by the Ethics Committee for Animal Use at Central Pharmacological Research Institute, Japan Tobacco Inc. Body weights were measured at 6, 10, 14, 18, and 22 weeks of age. Daily calorie intake was calculated from the average daily food intake (g/day) at 6, 10, 14, 18, and 22 weeks of age and calorie per weight of the normal diet (CRF-1; 3.57 kcal/g) and HFCC diet (D11061901; 4.80 kcal/g).

Tissue sampling and immunostaining

All animals were exsanguinated and dissected under isoflurane anesthesia at 22 weeks of age. Liver samples were collected for lipid content measurement, gene expression analysis, and histopathological evaluation. Intestinal samples were collected for gene expression analysis. Samples other than those used for pathological evaluation were stored at -80°C until use. Liver samples for pathological evaluation were fixed in 10% neutral-buffered formalin immediately after collection. The fixed tissues were paraffin-embedded and thinly sliced (3–5 μm). The prepared liver sections were stained with hematoxylin and eosin (H&E) or Sirius Red for pathological evaluation.

Hepatic lipid contents

The liver was removed from each rat and approximately 100 mg of each section was collected in tubes. Zirconia beads and methanol (0.5 mL) were added to the tube and the samples were homogenized using a model MM300 mixer mill (Retsch) at 25 Hz for 10 min. One milliliter of chloroform was added to all homogenates, mixed well, and centrifuged (10,000 × *g*, 5 min, 4°C) to extract lipids. Then, 0.2 mL of the supernatant was dried with nitrogen gas for approximately 40 min. The residue was redissolved in 0.5 mL 2-propanol and used for subsequent lipid measurements. Levels of TG, TC, PL, and non-esterified fatty acid (NEFA) in liver sections were measured using a model 3500 biochemistry automatic analyzer (Hitachi). Lipid hydroperoxide (LPO) content was determined using the LPO-CC kit (Kamiya Biomedical Company, Seattle, WA, USA) according to the manufacturer's protocol.

Biological parameters

Blood samples were collected from the tail vein of all rats at 6, 14, and 22 weeks of age for biochemical measurements of AST, ALT, GLU, TC, TG, and PL. These levels were measured using respective product kits (Roche Diagnostics, Tokyo, Japan) and an automatic analyzer (Hitachi).

RNA extraction and real-time quantitative PCR analysis

Total RNA was prepared from approximately 20 mg of liver or small intestine samples using the GenElute™ Mammalian Total RNA Miniprep Kit (MilliporeSigma), according to the manufacturer's protocols. Extracted RNA was suspended in DNAse/RNAse-free water and its concentration was measured using a NanoDrop spectrophotometer (Thermo Fisher Scientific, Waltham, MA, USA).

Reverse transcription of 1 μg of total RNA to complementary DNA (cDNA) was performed using the High-Capacity cDNA Reverse Transcription Kit with an RNase Inhibitor (Applied Biosystems) to synthesize cDNA. Reverse transcription reactions were performed using the following temperature and time cycles: 25°C for 10 min, 37°C for 120 min, and 85°C for 5 min.

Gene expression was quantified by real-time PCR using QuantStudio 7 Flex (Thermo Fisher Scientific) and TaqMan Gene Expression Assays (Table 2). The reaction mixture for real-time PCR contained 10 ng of cDNA. The temperature and time cycles were 10 min at 95°C, followed by 40 cycles of 15 s at 95°C, and 60 s at 60°C. The mRNA levels were calculated using *Gapdh* as the reference gene, and the expression levels in each group were corrected by the mean of the control group.

Statistical analyses

All values are expressed as mean ± standard deviation. The multiple-group test was performed as follows. Initially, equal variances were assessed using the Bartlett's test. The Tukey–Kramer method was used to analyze the homoscedasticity data. Otherwise, the Steel-Dwass method was used as a nonparametric test for heteroscedastic data. For all tests, statistical significance was set at $P<0.05$.

RESULTS

Weight change by HFCC or HFCC + CDX

The HFCC or HFCC+CDX loading period for female SD rats was set at 16 weeks. Female rats were chosen because CDX toxicity occurs at lower doses in male rats than in females [75]. During the study period, there was significant gain in body weight of rats in the HFCC group compared to that of rats in the control group from 14 to 18 weeks of age. In contrast, the HFCC+CDX group showed no weight gain compared with the control group throughout the study period (Fig. 6A). The daily caloric intake did not change in any of the groups throughout the study period (Fig. 6B). In addition, there was no evidence of overeating or significant obesity in this model.

Changes in blood biochemistry values by HFCC or HFCC+CDX

Eight weeks after the start of loading (14 weeks of age), blood AST levels were significantly increased only in the HFCC+CDX group (Fig. 6C). Significant increases were also evident in blood ALT, TC, and PL in both the HFCC and HFCC+CDX groups compared with the control group (Fig. 6D, F, H). At this point, excessive cholesterol

intake and liver damage began to occur. Blood GLU levels were slightly elevated in the HFCC group at 14 weeks of age but were not significantly different at 22 weeks of age (Fig. 6E). No significant changes were observed in the blood TG levels throughout the study period (Fig. 6G). At 16 weeks of loading (22 weeks of age), blood AST, ALT, TC, and PL levels were similar between the HFCC and HFCC+CDX groups. Both groups displayed significant increases or increasing trends compared to the control (Fig. 6C, D, F, H). Adequate cholesterol loading and hepatic injury were observed throughout the study.

Effects of cholesterol loading on liver weight and hepatic lipids

Analysis of liver lipid content revealed fatty liver formation as a major component of NAFLD pathogenesis. At 16 weeks after the start of loading (22 weeks of age), significant increases in hepatic TG, TC, NEFA, and LPO levels and liver weight per body weight were observed in the HFCC and HFCC+CDX groups compared to the control (Fig. 7A-C, E, F). Furthermore, hepatic PL content was significantly lower (Fig. 7D). Contrary to expectations, however, liver TC content did not increase in the HFCC+CDX group compared to that in the HFCC alone group (Fig. 7C). These results suggest that the HFCC diet induces hepatic lipid and cholesterol accumulation.

Liver histopathologic evaluation

Histopathological analysis of the liver is the most important evaluation method used to definitively diagnose NASH. I evaluated H&E-stained specimens for hepatosteatosis, hepatocyte hypertrophy, and inflammatory cell infiltration in the liver (Fig. 8A, Table 3). Animals in the control group showed no pathological changes in any of the parameters.

In contrast, all animals in the HFCC and HFCC+CDX groups showed fatty liver and inflammatory cell infiltration. Large lipid droplets in the liver, a hallmark of NASH pathology, tended to be observed more in animals in the HFCC+CDX group than in those in the HFCC group.

The degree of liver fibrosis is an important indicator that strongly correlates with the prognosis of patients with NASH. Sirius Red-stained specimens and analysis of the positive area fraction were used to evaluate the progression of liver fibrosis in all animals. Sirius Red staining of the tissue surrounding the vessel wall was stronger in animals in the HFCC group compared to the control group, but no significant change in the fibrosis area fraction was observed. In contrast, in the HFCC+CDX group, Sirius Red staining was observed between the liver parenchymal tissues and the fibrosis area ratio increased significantly (Fig. 8A, B). These results suggest that HFCC with CDX water intake might have caused more severe NASH pathogenesis than the HFCC diet alone.

Gene expression analysis in liver or intestinal tract

Fig. 9 shows the expression analysis results of NASH pathogenesis-related genes in the liver. The mRNA expression levels of lipid synthesis-related genes (*Srebp1*, *Scd1*, and *Pemt*), inflammation-related genes (*Tnf*, *Ccl2*, and *Il6*), and fibrosis-related genes (*Col1a1*, *Acta2*, and *Tgfb1*) were compared. Consistent with the results of changes in liver TG content (Fig. 7B), expression levels of the lipogenesis gene *Scd1* and its transcription factor *Srebp1* were significantly elevated in the HFCC and HFCC+CDX groups compared to the control (Fig. 9A, B). In contrast, the expression of *Pemt*, which plays an important role in phospholipid synthesis, decreased in the loaded groups (Fig. 9C), suggesting a possible influence on the decreased PL content in the liver. Compared to the

control group, upregulation of inflammation- and fibrosis-related gene expression in the liver was observed in both the HFCC and HFCC+CDX groups (Fig. 9D-I). In addition, the HFCC+CDX group tended to have a greater upregulation of inflammation-related genes than the HFCC group, although without a significant difference (Fig. 9D-F).

I then evaluated changes in the expression of genes related to cholesterol metabolism and ER stress in the liver and genes contributing to lipid absorption in the intestinal tract. There was a trend toward a decrease or significant decrease in hepatic *Srebp2* and gut *Npc1l1* mRNA expression in the HFCC and HFCC+CDX groups (Fig. 9J, O). The significant downregulation of hepatic *Fxr* in these groups (Fig. 9K) may contribute to the induction of NASH pathogenesis. Cholesterol accumulation in the liver causes liver damage, mainly through ER stress. The expression of the ER stress-related gene *Atf4* in the liver was elevated only in the HFCC+CDX group (Fig. 9M).

DISCUSSION

The lack of animal models that fully mimic human NASH pathology has hindered the understanding of the mechanisms of the disease. In addition, the long time required for NASH pathogenesis in animal models makes drug development difficult. In response to the lack of animal models of the disease, we validated the use of a cholesterol overload and absorption enhancement to create a new rat model of NASH that features faster and more severe disease formation. SD rats were fed a high-fat, high-cholesterol, and cholic acid-containing diet with CDX water. In a previous study, it was reported that HFCC+CDX loading in mice can induce NASH pathology with fatty liver, inflammation, and mild fibrosis within 3 weeks [73,74]. Accordingly, I subjected SD rats to this dietary

load to determine whether the pathophysiology could be made more severe compared to that in a simple cholesterol-induced NASH model.

The diet used in this study contained cholic acid. This bile acid is involved in the reduction of hepatic NEFA, TG, and VLDL synthesis via farnesoid X receptor (FXR) signaling. In addition, mice fed a high-fat diet containing cholic acid reportedly displayed inhibited body weight gain due to increased energy expenditure [76]. Thus, while cholic acid might improve NASH pathology, it can also increase cholesterol absorption in the intestinal tract and induce multiple collagen-related genes in the liver [77,78]. In rats, high-fat, cholesterol, and cholate diets have been reported to cause hyperlipidemia, hyperglycemia, and liver damage [79]. Cholic acid is often used in the diet to create NASH models. CDX is a cyclodextrin derivative with practical pharmaceutical, cosmetic, and industrial applications. CDX has hydrophobic cavities inside its ring structure, enabling the uptake organic compounds and other substances to increase their solubility. It has been suggested that the inclusion complex formation of CDX with cholesterol makes the latter more water-soluble than cholesterol alone [80], thereby promoting cholesterol absorption in the gut.

In this study, NASH-like pathogenesis of fatty liver and hepatitis was observed in all animals treated with HFCC or HFCC+CDX for 16 weeks. Elevated liver NEFA and LPO levels may contribute to liver injury from lipotoxicity and oxidative stress, respectively. Decreased hepatic PL is one of the features observed in NASH. In addition, Sirius Red staining of the liver tissue in the HFCC+CDX group revealed a significant increase in the fibrotic area fraction. The trend toward higher expression levels of liver inflammation-related gene markers in the HFCC+CDX group than in the HFCC group, together with significantly higher expression of ER stress-related genes, suggests that NASH pathology

was more potently induced by the presence of CDX. However, there was no significant difference in the liver TC content between the HFCC and HFCC+CDX groups. The cause of this discrepancy remains unclear. CDX-induced toxicity induced by oral intake in female rats has been previously studied. Oral CDX intake of 5000 mg/kg/day for 12 months resulted in increased body weight, leukocytosis, thrombocytopenia, and lung abnormalities, with no evidence of toxicity in the liver [75]. Therefore, it is unlikely that CDX-induced toxicity was the cause of the more severe NASH pathology that I observed in the HFCC+CDX group. Several data points led us to consider the possibility that there is a difference in the speed of pathogenesis. Eight weeks after the start of loading (14 weeks of age), blood AST and ALT levels were higher in the HFCC+CDX group. Preliminary studies also showed increased expression of liver inflammation- and fibrosis-related markers in the HFCC+CDX group at the same time point (8 weeks after the start of loading; data not shown). This suggests that accelerated cholesterol absorption in the CDX-loaded group might have contributed to an earlier plateau in hepatic cholesterol accumulation, leading to more severe NASH pathogenesis. Evaluations of liver TC content and other NASH-related parameters from early autopsies are needed to confirm this suggestion.

Despite increased expression of liver fibrosis-related genes in the HFCC group, histopathological analysis revealed no progression of liver fibrosis. This result seemingly contradicts the results of the histopathological evaluation of liver fibrosis. It is possible that HFCC alone induced liver fibrosis but did not reach a definite pathological stage.

Hydroxymethylglutaryl-CoA (HMG-CoA) reductase and low-density lipoprotein (LDL) receptor, which play important roles in cholesterol homeostasis in the liver, are regulated by sterol regulatory element-binding protein 2 (SREBP2). An important

pathway for cholesterol metabolism in the liver is its conversion to bile acids and their excretion, which is controlled by the FXR and other nuclear receptors. In the present study, the expression of these two key genes was significantly downregulated in the HFCC and HFCC+CDX groups. This may be a feedback response to the accumulation of cholesterol in the liver to inhibit its synthesis and uptake. The gene expression of *Fxr* is important for inhibiting cytotoxic bile acid synthesis and promoting efflux [81,82]. It is very likely that reduced *Fxr* activity contributes to cholesterol accumulation in the liver. In addition, FXR in hepatic stellate cells reportedly induces cell quiescence and apoptosis-promoting phenotypes that promote resolution of hepatic fibrosis [83]. The importance of FXR as a crucial nuclear receptor in NASH pathogenesis is evidenced by the many drugs targeting FXR that are being explored as NASH treatments. Reduced *Fxr* expression is an important feature of our novel animal model.

Similar to our study, several previous reports described NASH models in which rats were fed high-fat, high-cholesterol, and cholic acid diets [29,84]. Ichimura *et al.* described a diet composition similar to ours. The authors observed significantly decreased expression levels of *Srebp2* and *Fxr* as cholesterol- and bile acid-related genes in the liver, which is consistent with our results, while their model showed more advanced NASH pathology, including liver fibrosis [84]. The fact that the HFCC loading period of their animals was 2 weeks longer than ours might not be a sufficient explanation for this difference. I focused on differences in the pathogenesis of NASH between the sexes of rats. In our model, female SD rats were used to eliminate the toxic effects of orally ingesting CDX. It is well known that the incidence of NASH is higher in males than in females in humans [35]. This is considered to be due to the antimetabolic syndrome and hepatoprotective effects of female hormones [38]. I cannot rule out the possibility that the

limitation of using female rats to establish the NASH model might have resulted in milder NASH pathology compared to male rats subjected to a similar high-cholesterol load.

Compared to the typical NASH model, the CDAA diet model, the HFCC+CDX model takes a longer time to develop pathology, but the mechanisms of the two are different. The CDAA diet causes increased lipid synthesis in the rat liver and decreased TG secretion from the liver, leading to marked hepatic steatosis in a short period of time. In other words, the type of lipids that accumulate in the liver may be different from the HFCC+CDX model, in which cholesterol accumulation is predominant. In human NASH, a correlation between cholesterol and pathophysiology has been consistently reported [72], and the HFCC+CDX model may be a more useful and potentially a better model for studying NASH pathophysiology in the context of cholesterol.

In conclusion, I successfully induced NASH pathogenesis in female SD rats using HFCC diet loading. Addition of CDX in the diet aggravated this disease. These results suggest the possibility of a new NASH model that focuses on cholesterol overload and accelerated absorption.

Table 2 TaqMan Gene Expression Assays used for real-time PCR

Gene classification	Gene name	TaqMan ID
Liver lipid-related genes	*Scd1*	Rn06152614_s1
	Srebp1	Rn01495769_m1
	Srebp2	Rn01502638_m1
	Pemt	Rn00564517_m1
	Fxr	Rn00572658_m1
Liver fibrosis-related genes	*Col1a1*	Rn01463848_m1
	Acta2	Rn01759928_g1
	Tgfb1	Rn99999016_m1
Liver inflammation-related genes	*Tnf*	Rn99999017_m1
	Ccl2	Rn00580555_m1
	Il6	Rn01410330_m1
Liver ER stress-related genes	*Chop*	Rn00492098_g1
	Atf4	Rn00824644_g1
Gut absorption-related genes	*Cd36*	Rn00580728_m1
	Npc1l1	Rn01443503_m1
Endogenous control gene	*Gapdh*	Rn99999916_s1

Table 3 Histopathological findings in liver

	Control						HFCC						HFCC+CDX					
	1	2	3	4	5	6	1	2	3	4	5	6	1	2	3	4	5	6
Hepatosteatosis (Vacuolation/Fatty change)	–	–	–	–	–	–	±	±	+	+	±	±	±	+	+	±	+	2+
Hypertrophy of hepatocytes	–	–	–	–	–	–	+	+	+	+	±	±	±	+	±	+	+	+
Infiltration, inflammatory cells	–	–	–	–	–	–	±	+	±	±	±	±	+	+	±	±	±	±

–; Negative, ±; Very slight, +; Slight, 2+; Moderate, 3+; Severe

The results are the summary of pathological evaluation by H&E staining (hepatosteatosis, hypertrophy of hepatocytes, and infiltration of inflammatory cells) (n = 6).

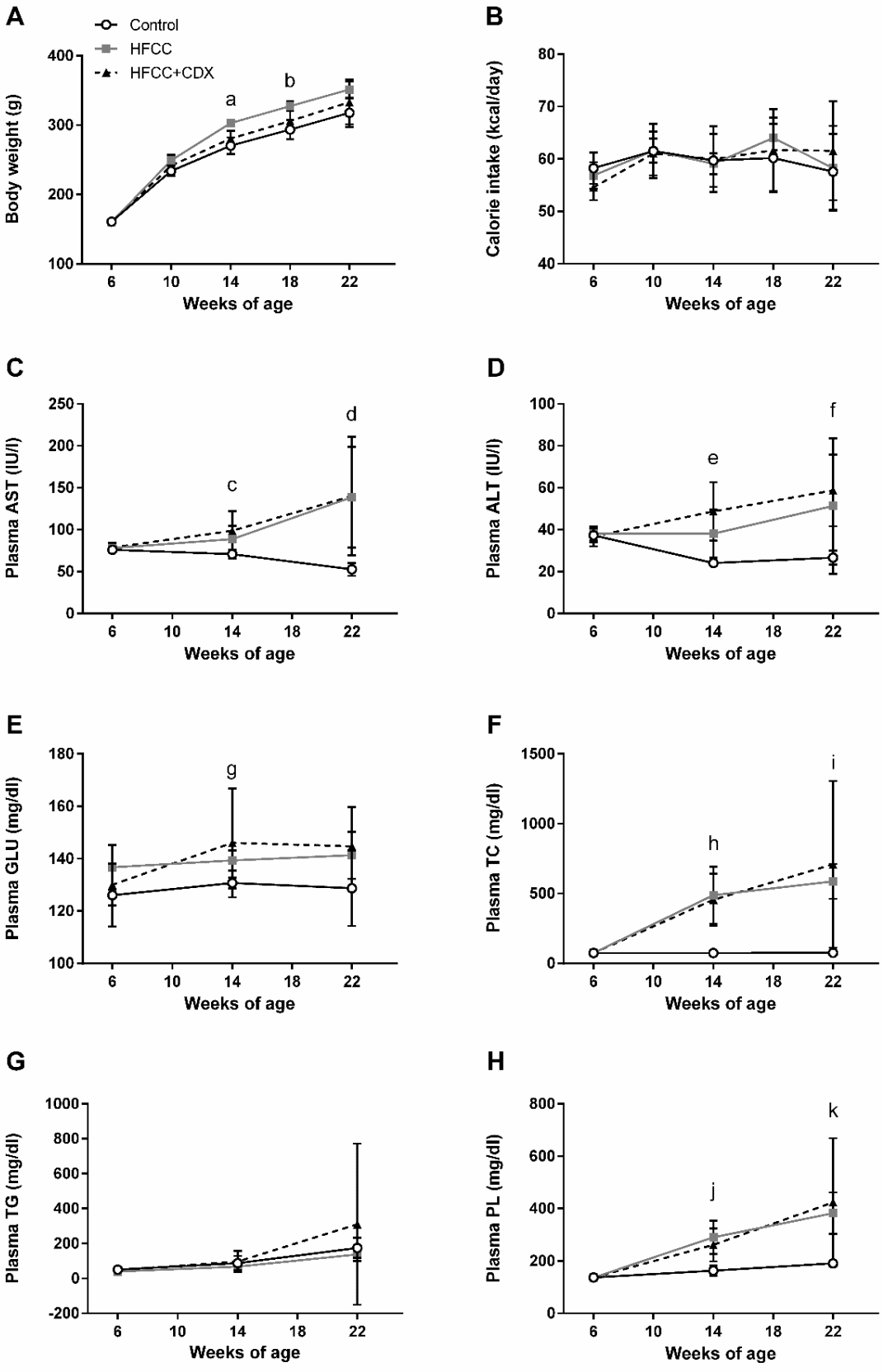
A
Control
HFCC
HFCC+CDX
Body weight (g)
400
300
200
100
a
b
6
10
14
18
22
Weeks of age
B
Calorie intake (kcal/day)
80
70
60
50
40
Weeks of age
C
Plasma AST (IU/l)
250
200
150
100
50
0
c
d
Weeks of age
D
Plasma ALT (IU/l)
100
80
60
40
20
0
e
f
Weeks of age
E
Plasma GLU (mg/dl)
180
160
140
120
100
g
Weeks of age
F
Plasma TC (mg/dl)
1500
1000
500
0
h
i
Weeks of age
G
Plasma TG (mg/dl)
1000
800
600
400
200
0
-200
Weeks of age
H
Plasma PL (mg/dl)
800
600
400
200
0
j
k
Weeks of age

Fig. 6 Body weight, daily caloric intake, and blood biochemical values

Data represent the mean ± standard deviation (n = 6). Letters in the graph (a-k) indicate significant differences at each point. #$P < 0.05$, ##$P < 0.01$, compared with the Tukey–Kramer method. $P<0.05, $$P<0.01, compared to the Steel-Dwass method.

(A) Body weight, **a:** ##$P < 0.01$ HFCC vs. control, ##$P < 0.01$ HFCC + CDX vs. HFCC, **b**: ##$P < 0.01$ HFCC vs. control, #$P < 0.05$ HFCC+CDX vs. HFCC

(B) Daily caloric intake, no significant differences between the groups at all time points.

(C) Plasma AST, **c**: $$P < 0.05$ HFCC+CDX vs. control, **d**: $$P < 0.05$ HFCC vs. control

(D) Plasma ALT, **e**: $$P < 0.05$ HFCC vs. control, $$$P < 0.01$ HFCC+ CDX vs. control, **f**: $$P < 0.05$ HFCC vs. control, $$P < 0.05$ HFCC+ CDX vs. control

(E) Plasma GLU, **g**: $$$P < 0.01$ HFCC vs. control

(F) Plasma TC, **h**: $$P < 0.05$ HFCC vs. control, $$P < 0.05$ HFCC+ CDX vs. control, **i**: $$P < 0.05$ HFCC vs. control, $$P < 0.05$ HFCC+ CDX vs. control,

(G) Plasma TG, no significant differences between the groups were evident at all time points.

(H) Plasma PL, **j:** HFCC vs. control, #$P < 0.01$ HFCC vs. control, **k:** $$P < 0.05$ HFCC+CDX vs. control, $$P < 0.05$ HFCC vs. control, $$P < 0.05$ HFCC+ CDX vs. control

HFCC: high-fat, high-cholesterol, and cholic acid diet; CDX: hydroxypropyl-β-cyclodextrin

AST: Aspartate transaminase, ALT: Alanine transaminase, GLU: Glucose,

TC: Total cholesterol, TG: Triglyceride, PL: Phospholipid

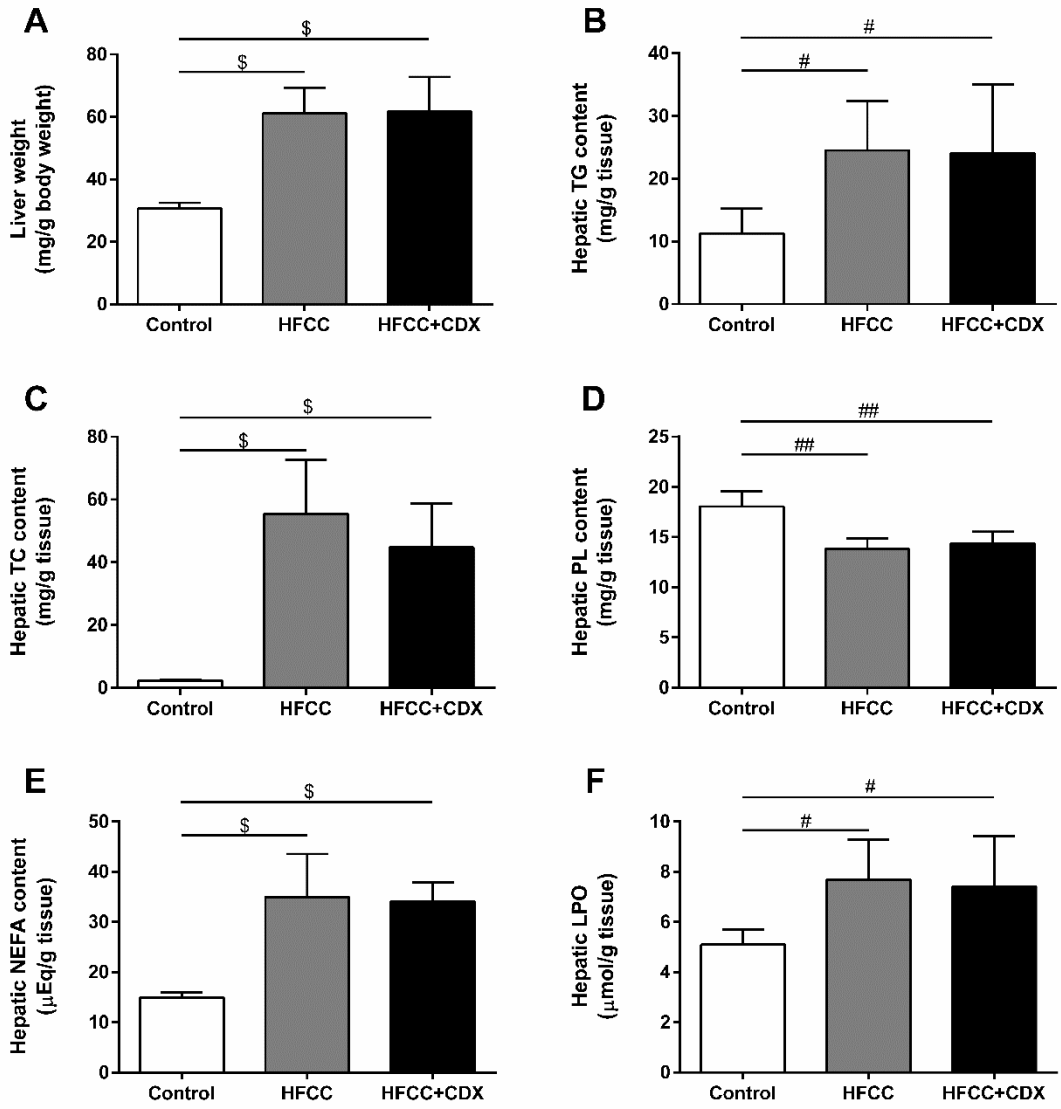

Fig. 7 Liver weight and liver lipid contents at 22 weeks of age

(A) Liver weight (mg) per g body weight, (B) Liver TG, (C) Liver TC, (D) Liver PL, (E) Liver NEFA, (F) Liver LPO

Data represent the mean ± standard deviation (n = 6). #P < 0.05, ##P < 0.01, compared using the Tukey-Kramer method. \$$P$ < 0.05, \$\$$P$ < 0.01, compared to the Steel-Dwass method.

TG: Triglyceride, TC: Total cholesterol, PL: Phospholipid, NEFA: Non-esterified fatty acid, LPO: Lipid hydroperoxide

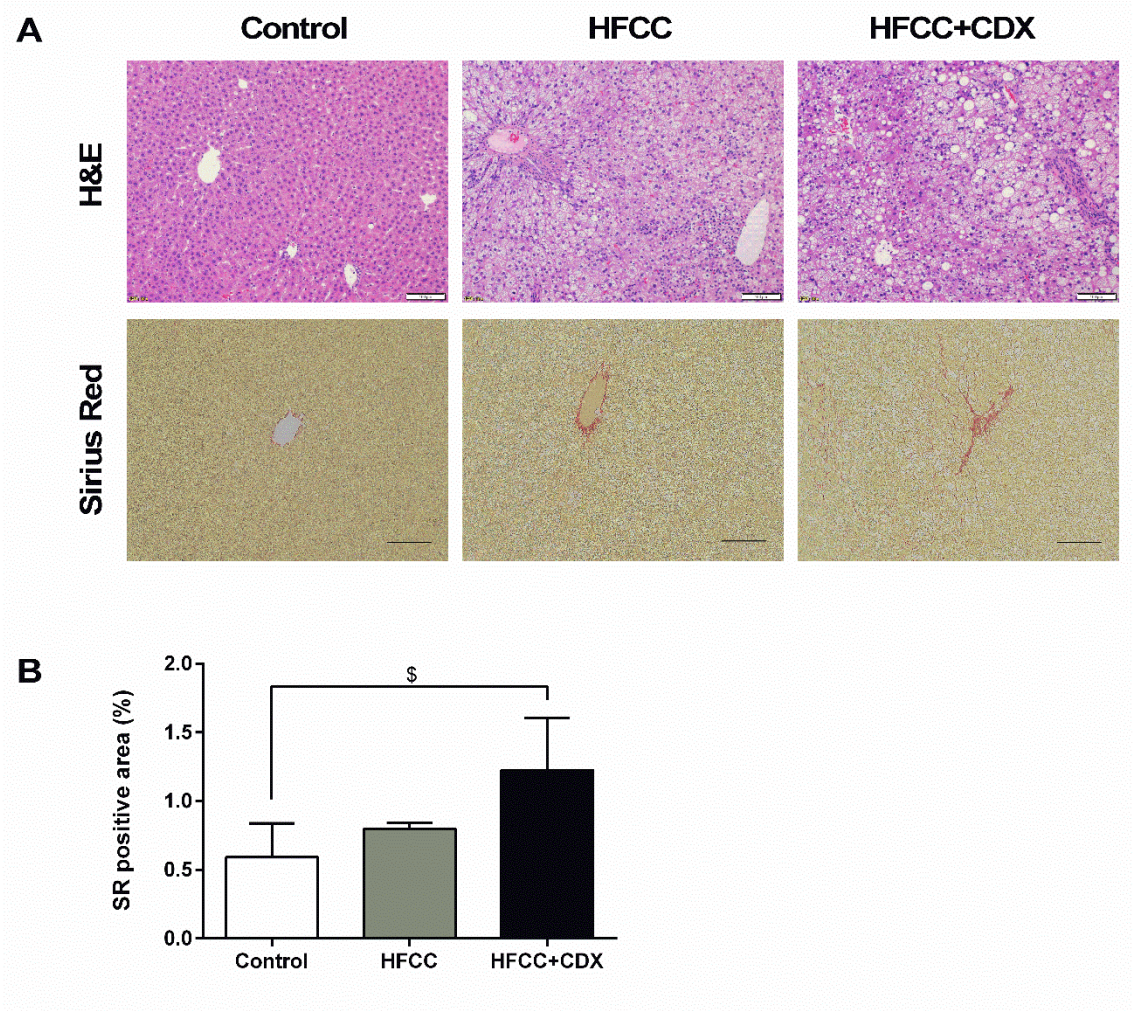

Fig. 8 Histopathology immunostaining of liver at 22 weeks of age

Representative pictures of stained specimens from each group of animals are shown.

(A) Upper panel: H&E staining of liver sections (Scale bars: 100 μm); lower panel: Sirius Red staining of liver sections (Scale bars: 100 μm).

(B) Sirius Red-positive area (%).

Data represent the mean ± standard deviation ($n = 6$). \$$P < 0.05$, compared to the Steel-Dwass method.

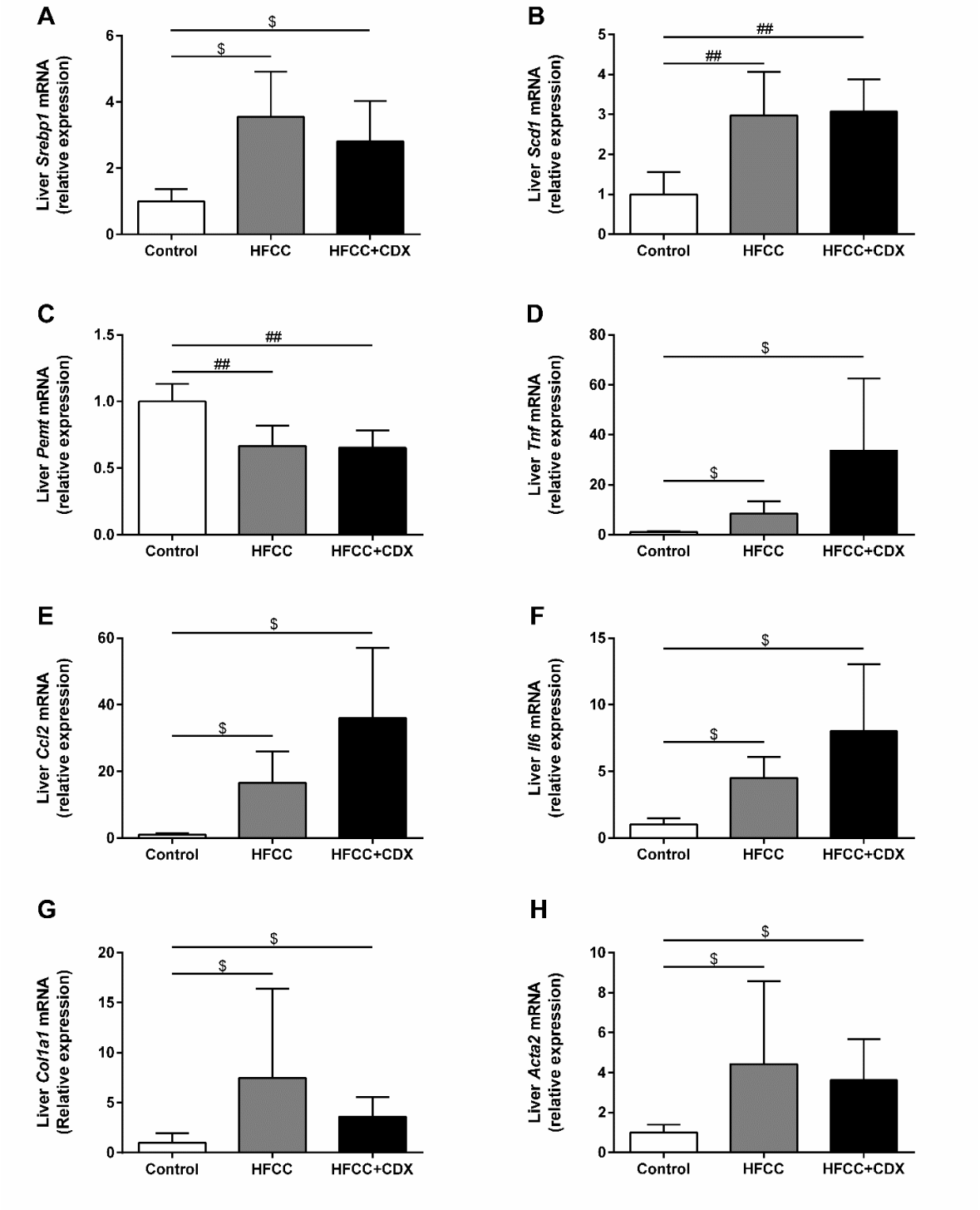
A
Liver Srebp1 mRNA (relative expression)
$
$
Control
HFCC
HFCC+CDX
B
Liver Scd1 mRNA (relative expression)
##
##
C
Liver Pemt mRNA (relative expression)
##
##
D
Liver Tnf mRNA (relative expression)
$
$
E
Liver Ccl2 mRNA (relative expression)
$
$
F
Liver Il6 mRNA (relative expression)
$
$
G
Liver Col1a1 mRNA (Relative expression)
$
$
H
Liver Acta2 mRNA (relative expression)
$
$

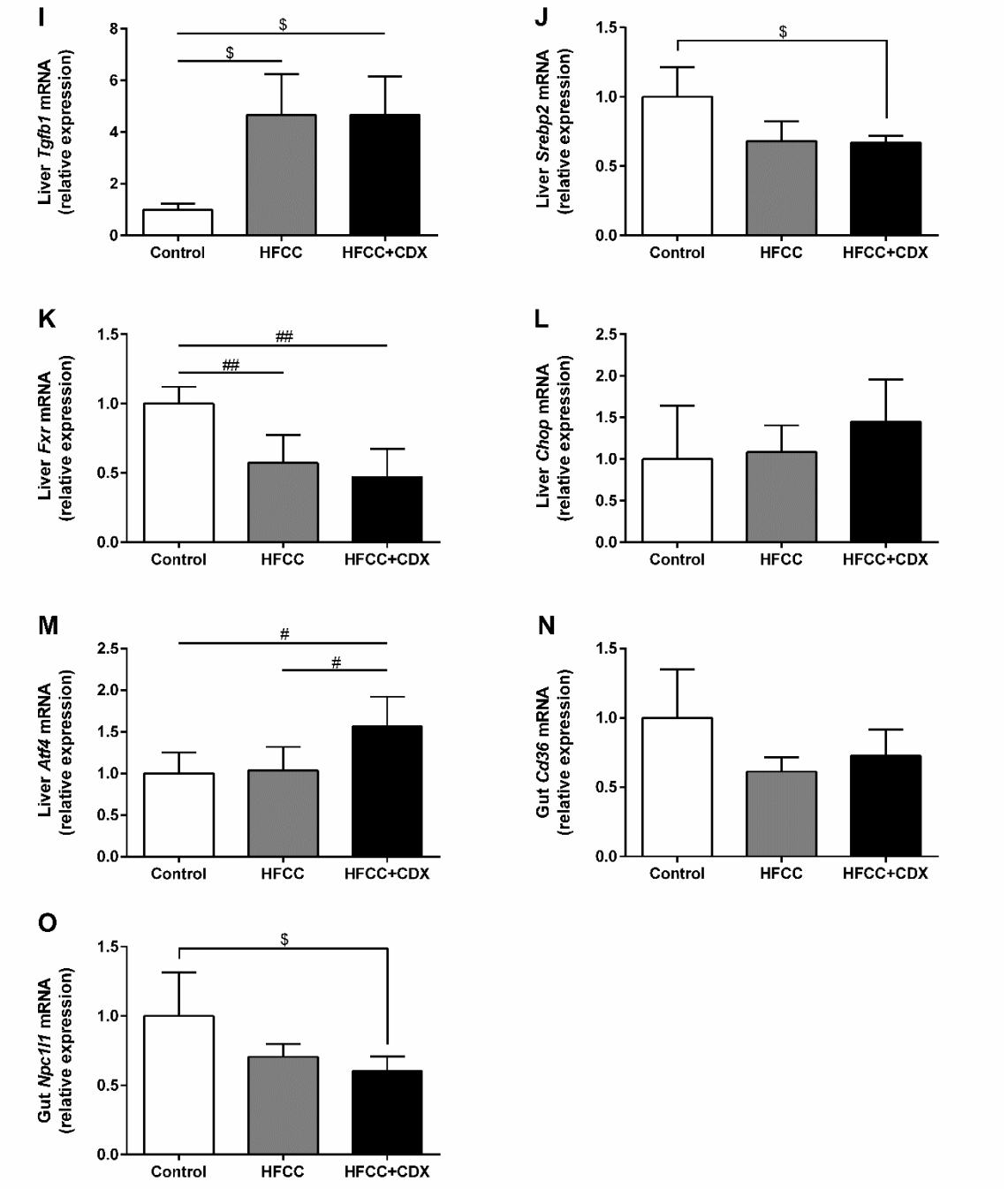

Fig. 9 Expression of genes related to lipid, inflammation, fibrosis, and ER stress in the liver and lipid absorption in the intestinal tract at 22 weeks of age

(A) Hepatic *Srebp1*, (B) Hepatic *Scd1*, (C) Hepatic *Pemt*, (D) Hepatic *Tnf*, (E) Hepatic *Ccl2*, (F) Hepatic *Il6*, (G) Hepatic *Col1a1*, (H) Hepatic *Acta2*, (I) Hepatic *Tgfb*, (J)

Hepatic *Srebp2*, (K) Hepatic *Fxr*, (L) Hepatic *Chop*, (M) Hepatic *Atf4*, (N) Gut *Cd36*, and (O) Gut *Npc1l1*

Data represent the mean ± standard deviation ($n = 6$). #$P < 0.05$, ##$P < 0.01$, compared using the Tukey-Kramer method. \$$P < 0.05$, compared using the Steel-Dwass method.

Chapter 4

General Discussion

Importance of Fibrosis in NASH Pathology

The phenotype of liver fibrosis is of great importance when animal models are used to evaluate new NASH therapeutics. This is because in longitudinal studies of human NAFLD patients, liver fibrosis stage, but not other histologic features of steatohepatitis, has been independently associated with long-term all-cause mortality, liver transplantation, and liver-related events [85]. The U.S. Food and Drug Administration (FDA) has provided clear guidance to the pharmaceutical industry on the development of drugs for the treatment of non-cirrhotic NASH with liver fibrosis (https://www.fda.gov/media/119044/download). According to this guidance, FDA approval of a drug for the treatment of NASH requires that the following endpoints be achieved in clinical trials: resolution of steatohepatitis on overall histopathological reading and no worsening of liver fibrosis on NASH Clinical Research Network (CRN) fibrosis score, or improvement in liver fibrosis greater than or equal to one stage (NASH CRN fibrosis score) and no worsening of steatohepatitis, or both resolution of steatohepatitis and improvement in fibrosis. The two animal models of NASH established in this study both show a significant increase in liver fibrosis area ratio, which may be useful in the development of novel therapies.

Sex Differences in NAFLD/NASH

Previous epidemiologic studies have shown clear sex differences in the incidence of NAFLD. Overall, the prevalence of NAFLD is higher in men than in women, and the age risk is higher in women than in men [86,87]. Hormonal treatment of postmenopausal

women also has a significant effect on improving NAFLD, suggesting that estrogen is protective against NAFLD. Estrogen's effect is to regulate many steps of lipid metabolism in the liver. Estrogen prevents fatty liver by reducing de novo lipogenesis. Insufficient estrogen signaling decreases VLDL secretion and promotes TG accumulation in the liver [88]. This same effect was observed in our OVX-induced NASH model. In mammalian females, estrogen receptors are highly expressed in the liver. Recent studies have shown that the liver responds differently in males and females to a high-lipid diet. In the male liver, lipid influx and synthesis are enhanced, leading to hepatic lipid accumulation. On the other hand, the female liver is able to inhibit the synthesis and absorption of excess lipids and promote fatty acid oxidation [89]. The cause of this sex difference may be attributed to differences in the expression of estrogen receptors in the liver. In rats, estrogen has been reported to suppress hepatic stellate cell activation and to inhibit the induction of hepatic fibrosis via estrogen receptors [90]. Combined with its effects on lipid metabolism, the impact of estrogen on NASH pathogenesis may be very large.

No significant gender difference in the prevalence of NAFLD exists in men and women over 50 years of age (23.6% vs. 24.2%) [91]. The decrease in female hormones due to menopause is thought to be a factor that may fill the gender gap in prevalence between men and women. However, with regard to NASH pathology in men and women over 50 years of age, women are at higher risk of developing advanced liver fibrosis than men [92]. Thus, NASH pathology differs in characteristics depending on sex and age, and the OVX-SDT fatty rats may be useful for elucidating the pathological mechanisms affecting the development of NASH in elderly women and for developing novel therapeutic strategies. However, despite the novelty of surgical induction of NASH, the pathophysiology of NASH was slower and milder than in existing animal models of

NASH. The endogenous factor of hormone depletion by OVX may have a milder effect on NASH induction than exogenous factors such as cholesterol overload. In other words, the long-term persistence of weak inflammatory changes in the liver may lead to the development of liver fibrosis. In addition, it is known that blood lipid parameters (TG, cholesterol) are elevated in perimenopausal women, so it is difficult to say that the model completely mimics the human condition in this point. In order to enhance the value of this model, more detailed studies on OVX-induced changes in the liver and other organs are needed.

Cholesterol Homeostasis in NASH

Multiple human studies consistently support a correlation between the development of NASH or cirrhosis and cholesterol intake [93–95]. Interestingly, a study examining nutritional factors in non-obese and obese NAFLD patients reported significantly higher dietary cholesterol intake in the non-obese group. At the same time, non-obese NAFLD patients do not necessarily have the other NAFLD risk factors found in obese patients, such as insulin resistance and abnormal adipocytokine secretion. This suggests that dietary cholesterol may play an important role in NAFLD formation [96]. As described in Chapter 3, important features of the HFCC+CDX NASH rat model established in this study are decreased hepatic *Srebp2* and *Fxr* expression and abnormal cholesterol homeostasis.

SREBP2 acts as a sensor of cholesterol depletion in the liver. Upon sensing cholesterol depletion, SREBP2 is activated and induces the expression of HMG-CoA reductase and LDL receptor. This response activates cholesterol synthesis and uptake in the liver [97]. Therefore, it is possible that *Srebp2* expression is suppressed in this model due to

excessive cholesterol accumulation in the liver, and that this suppresses the synthesis and uptake of cholesterol.

The function of FXR on cholesterol homeostasis is very complex. In the liver, FXR upregulates scavenger receptor class B type 1 and increases the uptake of HDL cholesterol from the blood. FXR also increases the expression of the ATP-binding cassette transporter G5 and G8 and promotes excretion of cholesterol and bile acids. It also interferes with the conversion of cholesterol to bile acids, increases β-oxidation, decreases fat synthesis, and promotes TG elimination [81,82,98,99]. The NASH drug development pipeline includes a number of FXR agonists. Some candidate compounds have been shown to be effective in improving human NASH. Therefore, it is likely that the reduction of *Fxr* expression due to cholesterol loading in this study has an adverse effect on NASH pathogenesis. More detailed studies will be needed to understand the full extent of the signaling changes in the liver caused by *Fxr* reduction.

In this study, I aimed to induce more severe NASH pathology by the addition of CDX to the HFCC alone-loaded NASH model. This objective was achieved, as HFCC+CDX increased liver fibrosis and tended to increase the expression of inflammatory markers compared to HFCC alone. However, the degree of NASH pathology is milder in this model than in the HFCC-loaded model using male rats. In the future, HFCC+CDX loading study in male SD rats may be necessary. In addition, it is virtually impossible to find this level of dietary cholesterol in human NASH patients. This difference from human NASH should be noted when using this model.

Ideal NAFLD/NASH Pathophysiology Model

An ideal animal model of disease, not only NAFLD/NASH, should mimic as much as

possible the characteristics of the disease in humans. In NAFLD/NASH, where the mechanisms of pathogenesis and pathological progression are not fully understood, it would be very useful to conduct studies using animal models with these characteristics to understand the disease. Even when used in non-clinical studies to confirm the effects of NASH drugs, the use of animal models that perfectly mimic human NASH pathology can increase the likelihood that NASH drugs will also improve the human disease [100]. In humans, however, the rate of progression from NAFL to NASH is not high (10-20%), and progression to cirrhosis and hepatocarcinoma takes more than 5 years. It is not realistic in terms of cost and time to use animal models that also mimic these characteristics for preclinical studies of drugs. The gold standard animal model for NASH should mimic the characteristics of human disease only in the mechanisms of onset and progression, and should develop NASH "rapidly," "with high probability," and "with a high degree of severity" from the start of loading. The inability to solve this difficult requirement is probably the reason why a gold standard model cannot be established in the NASH field. In fact, many animal models used in drug development only partially represent the characteristics of human NASH and are selected for their ability to demonstrate the metabolic improvement, anti-inflammatory, and anti-fibrosis effects of the drugs used. Therefore, it is important to establish a variety of animal models that can be used for a variety of purposes in order to advance NASH disease research and develop novel therapies. I studied the establishment of an unprecedented NASH pathophysiology model by surgical procedures or the updating of an existing high cholesterol load model by CDX water treatment. I hope that the findings of this study will help remedy the shortage of diverse animal models of NASH pathology.

Acknowledgements

I would like to thank Dr. Shigenori Ohkawa, Dr. Mutsuyoshi Matsushita and Dr. Takayuki Yamaguchi from Japan Tobacco Inc. Central Pharmaceutical Research Institute and Pharmaceutical Research Division for providing the opportunity to conduct this study. I would also like to express my gratitude to Dr. Tomohiko Sasase, who provided constructive comments and suggestions, and would also like to thank Mr. Yuichi Shinozaki, Dr. Tatsuya Maekawa, Mr. Ryuhei Sano, Dr. Yasufumi Toriniwa, Dr. Kinuko Uno, Miss. Marika Tohma, and Professor Katsuhiro Miyajima for their advice and involvement with parts of the experiments. I also wish to express my sincere graduate to Professor Takeshi Ohta from Kyoto University for providing helpful advice for the completion of this study.

References

1 Castaneda D, Gonzalez AJ, Alomari M, Tandon K, Zervos XB. From hepatitis A to E: A critical review of viral hepatitis. World J Gastroenterol. 2021 Apr;27(16):1691–715.

2 Karlsen TH, Folseraas T, Thorburn D, Vesterhus M. Primary sclerosing cholangitis - a comprehensive review. J Hepatol. 2017 Dec;67(6):1298–323.

3 Reshetnyak VI. Primary biliary cirrhosis: Clinical and laboratory criteria for its diagnosis. World J Gastroenterol. 2015 Jul;21(25):7683–708.

4 Sahebjam F, Vierling JM. Autoimmune hepatitis. Front Med. 2015 Jun;9(2):187–219.

5 Schonfeld EA, Brown RS. Genetic Causes of Liver Disease: When to Suspect a Genetic Etiology, Initial Lab Testing, and the Basics of Management. Med Clin North Am. 2019 Nov;103(6):991–1003.

6 Zhou W-C, Zhang Q-B, Qiao L. Pathogenesis of liver cirrhosis. World J Gastroenterol. 2014 Jun;20(23):7312–24.

7 Schaffner F, Thaler H. Nonalcoholic fatty liver disease. Prog Liver Dis. 1986;8:283–98.

8 Charlton MR, Burns JM, Pedersen RA, Watt KD, Heimbach JK, Dierkhising RA. Frequency and Outcomes of Liver Transplantation for Nonalcoholic Steatohepatitis in the United States. Gastroenterology. 2011 Oct;141(4):1249–53.

9 Farrell GC, Wong VW-S, Chitturi S. NAFLD in Asia--as common and important as

in the West. Nat Rev Gastroenterol Hepatol. 2013 May;10(5):307–18.

10 Abul-Husn NS, Cheng X, Li AH, Xin Y, Schurmann C, Stevis P, et al. A Protein-Truncating *HSD17B13* Variant and Protection from Chronic Liver Disease. N Engl J Med. 2018 Mar;378(12):1096–106.

11 Eslam M, Mangia A, Berg T, Chan HLY, Irving WL, Dore GJ, et al. Diverse impacts of the rs58542926 E167K variant in TM6SF2 on viral and metabolic liver disease phenotypes. Hepatology. 2016 Jul;64(1):34–46.

12 Eslam M, George J. Genetic contributions to NAFLD: leveraging shared genetics to uncover systems biology. Nat Rev Gastroenterol Hepatol. 2020 Jan;17(1):40–52.

13 Kozlitina J, Smagris E, Stender S, Nordestgaard BG, Zhou HH, Tybjærg-Hansen A, et al. Exome-wide association study identifies a TM6SF2 variant that confers susceptibility to nonalcoholic fatty liver disease. Nat Genet. 2014 Apr;46(4):352–6.

14 Romeo S, Kozlitina J, Xing C, Pertsemlidis A, Cox D, Pennacchio LA, et al. Genetic variation in PNPLA3 confers susceptibility to nonalcoholic fatty liver disease. Nat Genet. 2008 Dec;40(12):1461–5.

15 Oniki K, Saruwatari J, Izuka T, Kajiwara A, Morita K, Sakata M, et al. Influence of the PNPLA3 rs738409 Polymorphism on Non-Alcoholic Fatty Liver Disease and Renal Function among Normal Weight Subjects. PLoS ONE. 2015 Jul;10(7):e0132640.

16 Matteoni CA, Younossi ZM, Gramlich T, Boparai N, Liu YC, McCullough AJ. Nonalcoholic fatty liver disease: a spectrum of clinical and pathological severity.

Gastroenterology. 1999 Jun;116(6):1413–9.

17 Younossi ZM, Stepanova M, Rafiq N, Makhlouf H, Younoszai Z, Agrawal R, et al. Pathologic criteria for nonalcoholic steatohepatitis: interprotocol agreement and ability to predict liver-related mortality. Hepatology. 2011 Jun;53(6):1874–82.

18 Brunt EM, Janney CG, Di Bisceglie AM, Neuschwander-Tetri BA, Bacon BR. Nonalcoholic steatohepatitis: a proposal for grading and staging the histological lesions. Am J Gastroenterol. 1999 Sep;94(9):2467–74.

19 Kleiner DE, Brunt EM, Van Natta M, Behling C, Contos MJ, Cummings OW, et al. Design and validation of a histological scoring system for nonalcoholic fatty liver disease. Hepatology. 2005 Jun;41(6):1313–21.

20 Bedossa P, FLIP Pathology Consortium. Utility and appropriateness of the fatty liver inhibition of progression (FLIP) algorithm and steatosis, activity, and fibrosis (SAF) score in the evaluation of biopsies of nonalcoholic fatty liver disease. Hepatology. 2014 Aug;60(2):565–75.

21 Nascimbeni F, Bedossa P, Fedchuk L, Pais R, Charlotte F, Lebray P, et al. Clinical validation of the FLIP algorithm and the SAF score in patients with non-alcoholic fatty liver disease. J Hepatol. 2020 May;72(5):828–38.

22 Sumida Y, Yoneda M. Current and future pharmacological therapies for NAFLD/NASH. J Gastroenterol. 2018 Mar;53(3):362–76.

23 Romero FA, Jones CT, Xu Y, Fenaux M, Halcomb RL. The Race to Bash NASH: Emerging Targets and Drug Development in a Complex Liver Disease. J Med Chem.

2020 May;63(10):5031–73.

24 C Y Fan, J Pan, N Usuda, A V Yeldandi, M S Rao, J K Reddy. Steatohepatitis, spontaneous peroxisome proliferation and liver tumors in mice lacking peroxisomal fatty acyl-CoA oxidase. Implications for peroxisome proliferator-activated receptor alpha natural ligand metabolism. The Journal of biological chemistry. 1998 Jun;273(25):15639-45.

25 Lindström P. The physiology of obese-hyperglycemic mice [ob/ob mice]. ScientificWorldJournal. 2007 May;7:666–85.

26 Okumura K, Ikejima K, Kon K, Abe W, Yamashina S, Enomoto N, et al. Exacerbation of dietary steatohepatitis and fibrosis in obese, diabetic KK-A(y) mice. Hepatol Res. 2006 Nov;36(3):217–28.

27 Shimomura I, Hammer RE, Richardson JA, Ikemoto S, Bashmakov Y, Goldstein JL, et al. Insulin resistance and diabetes mellitus in transgenic mice expressing nuclear SREBP-1c in adipose tissue: model for congenital generalized lipodystrophy. Genes Dev. 1998 Oct;12(20):3182–94.

28 Trak-Smayra V, Paradis V, Massart J, Nasser S, Jebara V, Fromenty B. Pathology of the liver in obese and diabetic ob/ob and db/db mice fed a standard or high-calorie diet. Int J Exp Pathol. 2011 Dec;92(6):413–21.

29 Horai Y, Utsumi H, Ono Y, Kishimoto T, Ono Y, Fukunari A. Pathological characterization and morphometric analysis of hepatic lesions in SHRSP5/Dmcr, an experimental non-alcoholic steatohepatitis model, induced by high-fat and high-

cholesterol diet. Int J Exp Pathl. 2016 Feb;97(1):75–85.

30 L L. Non-alcoholic fatty liver disease (NAFLD): a tale of fat and sugar? Fibrogenesis & tissue repair. 2013 Jul 18;6(1):14.

31 Okishio S, Yamaguchi K, Ishiba H, Tochiki N, Yano K, Takahashi A, et al. PPARα agonist and metformin co-treatment ameliorates NASH in mice induced by a choline-deficient, amino acid-defined diet with 45% fat. Sci Rep. 2020 Nov;10(1):19578.

32 Rinella ME, Elias MS, Smolak RR, Fu T, Borensztajn J, Green RM. Mechanisms of hepatic steatosis in mice fed a lipogenic methionine choline-deficient diet. J Lipid Res. 2008 May;49(5):1068–76.

33 Friedman SL, Neuschwander-Tetri BA, Rinella M, Sanyal AJ. Mechanisms of NAFLD development and therapeutic strategies. Nat Med. 2018 Jul;24(7):908–22.

34 Pais R, Maurel T. Natural History of NAFLD. J Clin Med. 2021 Mar 10;10(6):1161.

35 Lonardo A, Nascimbeni F, Ballestri S, Fairweather D, Win S, Than TA, et al. Sex Differences in Nonalcoholic Fatty Liver Disease: State of the Art and Identification of Research Gaps. Hepatology. 2019;70(4):1457–69.

36 Sarkar MA, Suzuki A, Abdelmalek MF, Yates KP, Wilson LA, Bass NM, et al. Testosterone is Associated With Nonalcoholic Steatohepatitis and Fibrosis in Premenopausal Women With NAFLD. Clinical Gastroenterology and Hepatology. 2021 Jun;19(6):1267-1274.e1.

37 DiStefano JK. NAFLD and NASH in Postmenopausal Women: Implications for

Diagnosis and Treatment. Endocrinology. 2020 Oct 1;161(10):bqaa134.

38 Farruggio S, Cocomazzi G, Marotta P, Romito R, Surico D, Calamita G, et al. Genistein and 17β-Estradiol Protect Hepatocytes from Fatty Degeneration by Mechanisms Involving Mitochondria, Inflammasome and Kinases Activation | Cell Physiol Biochem. Cellular Physiology & Biochemistry. 2020 Apr;54(3):401–16.

39 Nadal-Casellas A, Proenza AM, Lladó I, Gianotti M. Sex-dependent differences in rat hepatic lipid accumulation and insulin sensitivity in response to diet-induced obesity. Biochem Cell Biol. 2012 Apr;90(2):164–72.

40 Stöppeler S, Palmes D, Fehr M, Hölzen JP, Zibert A, Siaj R, et al. Gender and strain-specific differences in the development of steatosis in rats. Lab Anim. 2013 Jan;47(1):43–52.

41 Perry AC, Martin L. Race differences in obesity and its relationship to the sex hormone milieu. Horm Mol Biol Clin Investig. 2014 Sep;19(3):151–61.

42 Shepard BD. Sex differences in diabetes and kidney disease: mechanisms and consequences. Am J Physiol Renal Physiol. 2019 Aug;317(2):F456–62.

43 Masuyama T, Katsuda Y, Shinohara M. A Novel Model of Obesity-Related Diabetes: Introgression of the *Lepr*^{fa} Allele of the Zucker Fatty Rat into Nonobese Spontaneously Diabetic Torii (SDT) Rats. Experimental Animals. 2005;54(1):13–20.

44 Ishii Y, Motohashi Y, Muramatsu M, Katsuda Y, Miyajima K, Sasase T, et al. Female spontaneously diabetic Torii fatty rats develop nonalcoholic steatohepatitis-like hepatic lesions. World J Gastroenterol. 2015 Aug;21(30):9067–78.

45 Tilg H, Moschen AR, Roden M. NAFLD and diabetes mellitus. Nat Rev Gastroenterol Hepatol. 2017 Jan;14(1):32–42.

46 Fukui M, Senmaru T, Hasegawa G, Yamazaki M, Asano M, Kagami Y, et al. 17β-Estradiol attenuates saturated fatty acid diet-induced liver injury in ovariectomized mice by up-regulating hepatic senescence marker protein-30. Biochemical and Biophysical Research Communications. 2011 Nov;415(2):252–7.

47 Kanaya N, Kubo M, Liu Z, Chu P, Wang C, Yate-Ching Yuan SC. Protective Effects of White Button Mushroom (Agaricus bisporus) against Hepatic Steatosis in Ovariectomized Mice as a Model of Postmenopausal Women. PLOS ONE. 2011 Oct;6(10):e26654.

48 Kamada Y, Matsumoto H, Tamura S, Fukushima J, Kiso S, Fukui K, et al. Hypoadiponectinemia accelerates hepatic tumor formation in a nonalcoholic steatohepatitis mouse model. Journal of Hepatology. 2007 Oct;47(4):556–64.

49 Matsumoto M, Hada N, Sakamaki Y, Uno A, Shiga T, Tanaka C, et al. An improved mouse model that rapidly develops fibrosis in non-alcoholic steatohepatitis. International Journal of Experimental Pathology. 2013;94(2):93–103.

50 Ibrahim SH, Hirsova P, Malhi H, Gores GJ. Animal Models of Nonalcoholic Steatohepatitis: Eat, Delete, and Inflame. Dig Dis Sci. 2016 May;61(5):1325–36.

51 Scholten D, Trebicka J, Liedtke C, Weiskirchen R. The carbon tetrachloride model in mice. Lab Anim. 2015 Apr;49(1 Suppl):4–11.

52 Ishii Y, Ohta T, Sasase T, Morinaga H, Ueda N, Hata T, et al. Pathophysiological

analysis of female Spontaneously Diabetic Torii fatty rats. Exp Anim. 2010;59(1):73–84.

53 Blasiole DA, Davis RA, Attie AD. The physiological and molecular regulation of lipoprotein assembly and secretion. Mol Biosyst. 2007 Sep;3(9):608–19.

54 Resseguie M, Song J, Niculescu MD, Costa K-A da, Randall TA, Zeisel SH. Phosphatidylethanolamine N-methyltransferase (PEMT) gene expression is induced by estrogen in human and mouse primary hepatocytes. The FASEB Journal. 2007;21(10):2622–32.

55 Nakatsuka A, Matsuyama M, Yamaguchi S, Katayama A, Eguchi J, Murakami K, et al. Insufficiency of phosphatidylethanolamine N-methyltransferase is risk for lean non-alcoholic steatohepatitis. Sci Rep. 2016 Feb;6:21721.

56 Barsalani R, Chapados NA, Lavoie J-M. Hepatic VLDL-TG production and MTP gene expression are decreased in ovariectomized rats: effects of exercise training. Horm Metab Res. 2010 Nov;42(12):860–7.

57 Hata T, Ohta T, Ishii Y, Sasase T, Yamaguchi T, Mera Y, et al. Elevated glucagon-like peptide-1 on a high-fat diet feeding prevents the incidence of diabetes mellitus in Spontaneously Diabetic Torii *Lepr*^{fa} rats. 2012 May;2(2): 170-178

58 Estes C, Razavi H, Loomba R, Younossi Z, Sanyal AJ. Modeling the epidemic of nonalcoholic fatty liver disease demonstrates an exponential increase in burden of disease: Estes et al. Hepatology. 2018 Jan;67(1):123–33.

59 Younossi ZM, Koenig AB, Abdelatif D, Fazel Y, Henry L, Wymer M. Global

epidemiology of nonalcoholic fatty liver disease-Meta-analytic assessment of prevalence, incidence, and outcomes. Hepatology. 2016 Jul;64(1):73–84.

60 Sheka AC, Adeyi O, Thompson J, Hameed B, Crawford PA, Ikramuddin S. Nonalcoholic Steatohepatitis: A Review. JAMA. 2020 Mar;323(12):1175.

61 Fang Y-L, Chen H, Wang C-L, Liang L. Pathogenesis of non-alcoholic fatty liver disease in children and adolescence: From "two hit theory" to "multiple hit model." WJG. 2018 Jul;24(27):2974–83.

62 Buzzetti E, Pinzani M, Tsochatzis EA. The multiple-hit pathogenesis of non-alcoholic fatty liver disease (NAFLD). Metabolism. 2016 Aug;65(8):1038–48.

63 Eslam M, Sanyal AJ, George J, Sanyal A, Neuschwander-Tetri B, Tiribelli C, et al. MAFLD: A Consensus-Driven Proposed Nomenclature for Metabolic Associated Fatty Liver Disease. Gastroenterology. 2020 May;158(7):1999-2014.e1.

64 Lonardo A, Leoni S, Alswat KA, Fouad Y. History of Nonalcoholic Fatty Liver Disease. Int J Mol Sci. 2020 Aug;21(16):E5888.

65 Chaney A. Obesity and Nonalcoholic Fatty Liver Disease. Nurs Clin North Am. 2021 Dec;56(4):543–52.

66 Luo Y, Lin H. Inflammation initiates a vicious cycle between obesity and nonalcoholic fatty liver disease. Immun Inflamm Dis. 2021 Mar;9(1):59–73.

67 Younossi ZM, Golabi P, de Avila L, Paik JM, Srishord M, Fukui N, et al. The global epidemiology of NAFLD and NASH in patients with type 2 diabetes: A systematic

review and meta-analysis. Journal of Hepatology. 2019 Oct;71(4):793–801.

68 Xu Y, Yang X, Bian H, Xia M. Metabolic dysfunction associated fatty liver disease and coronavirus disease 2019: clinical relationship and current management. Lipids Health Dis. 2021 Dec;20(1):126.

69 Lee WM, Bae JH, Chang Y, Lee SH, Moon JE, Jeong SW, et al. Effect of Nutrition Education in NAFLD Patients Undergoing Simultaneous Hyperlipidemia Pharmacotherapy: A Randomized Controlled Trial. Nutrients. 2021 Dec;13(12):4453.

70 Byrne CD, Targher G. NAFLD as a driver of chronic kidney disease. Journal of Hepatology. 2020 Apr;72(4):785–801.

71 Febbraio MA, Reibe S, Shalapour S, Ooi GJ, Watt MJ, Karin M. Preclinical Models for Studying NASH-Driven HCC: How Useful Are They? Cell Metabolism. 2019 Jan;29(1):18–26.

72 Horn CL, Morales AL, Savard C, Farrell GC, Ioannou GN. Role of Cholesterol-Associated Steatohepatitis in the Development of NASH. Hepatol Commun. 2021;6(1)12–35.

73 Duparc T, Briand F, Trenteseaux C, Merian J, Combes G, Najib S, et al. Liraglutide improves hepatic steatosis and metabolic dysfunctions in a 3-week dietary mouse model of nonalcoholic steatohepatitis. Am J Physiol Gastrointest Liver Physiol. 2019 Oct;317(4):G508–17.

74 Briand F, Heymes C, Bonada L, Angles T, Charpentier J, Branchereau M, et al. A 3-week nonalcoholic steatohepatitis mouse model shows elafibranor benefits on hepatic

inflammation and cell death. Clin Transl Sci. 2020 May;13(3):529–38.

75 Gould S, Scott RC. 2-Hydroxypropyl-β-cyclodextrin (HP-β-CD): A toxicology review. Food and Chemical Toxicology. 2005 Oct;43(10):1451–9.

76 Watanabe M, Houten SM, Mataki C, Christoffolete MA, Kim BW, Sato H, et al. Bile acids induce energy expenditure by promoting intracellular thyroid hormone activation. Nature. 2006 Jan;439(7075):484–9.

77 Murphy C, Parini P, Wang J, Björkhem I, Eggertsen G, Gåfvels M. Cholic acid as key regulator of cholesterol synthesis, intestinal absorption and hepatic storage in mice. Biochim Biophys Acta. 2005 Aug;1735(3):167–75.

78 Vergnes L, Phan J, Strauss M, Tafuri S, Reue K. Cholesterol and cholate components of an atherogenic diet induce distinct stages of hepatic inflammatory gene expression. J Biol Chem. 2003 Oct;278(44):42774–84.

79 Jamshed H, Arslan J, Gilani A-H. Cholesterol-cholate-butterfat diet offers multi-organ dysfunction in rats. Lipids Health Dis. 2014 Dec;13:194.

80 Williams III RO, Mahaguna V, Sriwongjanya M. Characterization of an inclusion complex of cholesterol and hydroxypropyl-β-cyclodextrin. European Journal of Pharmaceutics and Biopharmaceutics. 1998 Nov;46(3):355–60.

81 Li T, Matozel M, Boehme S, Kong B, Nilsson L-M, Guo G, et al. Overexpression of cholesterol 7α-hydroxylase promotes hepatic bile acid synthesis and secretion and maintains cholesterol homeostasis. Hepatology. 2011 Mar;53(3):996–1006.

82 Lambert G, Amar MJA, Guo G, Brewer HB, Gonzalez FJ, Sinal CJ. The farnesoid X-receptor is an essential regulator of cholesterol homeostasis. J Biol Chem. 2003 Jan;278(4):2563–70.

83 Fiorucci S, Rizzo G, Antonelli E, Renga B, Mencarelli A, Riccardi L, et al. A farnesoid x receptor-small heterodimer partner regulatory cascade modulates tissue metalloproteinase inhibitor-1 and matrix metalloprotease expression in hepatic stellate cells and promotes resolution of liver fibrosis. J Pharmacol Exp Ther. 2005 Aug;314(2):584–95.

84 Ichimura M, Masuzumi M, Kawase M, Sakaki M, Tamaru S, Nagata Y, et al. A diet-induced Sprague–Dawley rat model of nonalcoholic steatohepatitis-related cirrhosis. The Journal of Nutritional Biochemistry. 2017 Feb;40:62–9.

85 Sanyal AJ, Van Natta ML, Clark J, Neuschwander-Tetri BA, Diehl A, Dasarathy S, et al. Prospective Study of Outcomes in Adults with Nonalcoholic Fatty Liver Disease. N Engl J Med. 2021 Oct;385(17):1559–69.

86 Fang JG, Zhu J, Li XJ, Li R, Dai F, Song XM, et al. [Epidemiological survey of prevalence of fatty liver and its risk factors in a general adult population of Shanghai]. Zhonghua Gan Zang Bing Za Zhi. 2005 Feb;13(2):83–8.

87 Hamaguchi M, Kojima T, Ohbora A, Takeda N, Fukui M, Kato T. Aging is a risk factor of nonalcoholic fatty liver disease in premenopausal women. World J Gastroenterol. 2012 Jan;18(3):237–43.

88 Palmisano BT, Zhu L, Stafford JM. Role of Estrogens in the Regulation of Liver Lipid

Metabolism. Adv Exp Med Biol. 2017;1043:227–56.

89 Meda C, Barone M, Mitro N, Lolli F, Pedretti S, Caruso D, et al. Hepatic ERα accounts for sex differences in the ability to cope with an excess of dietary lipids. Mol Metab. 2020 Feb;32:97–108.

90 Zhang B, Zhang C-G, Ji L-H, Zhao G, Wu Z-Y. Estrogen receptor β selective agonist ameliorates liver cirrhosis in rats by inhibiting the activation and proliferation of hepatic stellate cells. J Gastroenterol Hepatol. 2018 Mar;33(3):747–55.

91 Park SH, Jeon WK, Kim SH, Kim HJ, Park DI, Cho YK, et al. Prevalence and risk factors of non-alcoholic fatty liver disease among Korean adults. J Gastroenterol Hepatol. 2006 Jan;21(1 Pt 1):138–43.

92 Balakrishnan M, Patel P, Dunn-Valadez S, Dao C, Khan V, Ali H, et al. Women Have a Lower Risk of Nonalcoholic Fatty Liver Disease but a Higher Risk of Progression vs Men: A Systematic Review and Meta-analysis. Clin Gastroenterol Hepatol. 2021 Jan;19(1):61-71.e15.

93 Allard JP, Aghdassi E, Mohammed S, Raman M, Avand G, Arendt BM, et al. Nutritional assessment and hepatic fatty acid composition in non-alcoholic fatty liver disease (NAFLD): a cross-sectional study. J Hepatol. 2008 Feb;48(2):300–7.

94 Mokhtari Z, Poustchi H, Eslamparast T, Hekmatdoost A. Egg consumption and risk of non-alcoholic fatty liver disease. World J Hepatol. 2017 Apr;9(10):503–9.

95 Noureddin M, Zelber-Sagi S, Wilkens LR, Porcel J, Boushey CJ, Le Marchand L, et al. Diet Associations With Nonalcoholic Fatty Liver Disease in an Ethnically Diverse

Population: The Multiethnic Cohort. Hepatology. 2020 Jun;71(6):1940–52.

96 Yasutake K, Nakamuta M, Shima Y, Ohyama A, Masuda K, Haruta N, et al. Nutritional investigation of non-obese patients with non-alcoholic fatty liver disease: the significance of dietary cholesterol. Scand J Gastroenterol. 2009;44(4):471–7.

97 Radhakrishnan A, Goldstein JL, McDonald JG, Brown MS. Switch-like control of SREBP-2 transport triggered by small changes in ER cholesterol: a delicate balance. Cell Metab. 2008 Dec;8(6):512–21.

98 Yang Z-X, Shen W, Sun H. Effects of nuclear receptor FXR on the regulation of liver lipid metabolism in patients with non-alcoholic fatty liver disease. Hepatol Int. 2010 Aug;4(4):741–8.

99 Yu L, Gupta S, Xu F, Liverman ADB, Moschetta A, Mangelsdorf DJ, et al. Expression of ABCG5 and ABCG8 is required for regulation of biliary cholesterol secretion. J Biol Chem. 2005 Mar;280(10):8742–7.

100 Santhekadur PK, Kumar DP, Sanyal AJ. Preclinical models of non-alcoholic fatty liver disease. J Hepatol. 2018 Feb;68(2):230–7.